“SYNTHESIS AND PARAMETRIC OPTIMIZATION OF NICKEL-COBALT-PHOSPHORUS-TITANIUM DIOXIDE ELECTROLESS COATING”

THESIS SUBMITTED IN PARTIAL FULFILMENT OF THE REQUIREMENT FOR THE DEGREE OF

MASTER OF MECHANICAL ENGINEERING

IN

FACULTY OF ENGINEERING & TECHNOLOGY,
JADAVPUR UNIVERSITY

Submitted by

NILADRI SEKHAR DOLUI

Exam Roll No: M4MEC24013
Registration No: 163715 of 2022-2023

Under the Guidance of
Dr. Nabendu Ghosh
Mr. Abhishek Mandal

DEPARTMENT OF MECHANICAL ENGINEERING
JADAVPUR UNIVERSITY
KOLKATA – 700 032
MAY 2024

JADAVPUR UNIVERSITY

FACULTY OF ENGINEERING AND TECHNOLOGY

CERTIFICATE OF RECOMMENDATION

*We hereby recommend that the thesis prepared under our supervision by Niladri Sekhar Dolui, entitled, **"Synthesis and Parametric Optimization of Nickel-Cobalt-Phosphorus-Titanium Dioxide Electroless Coating"** be accepted in partial fulfilment of the requirements for awarding the degree of Master of Mechanical Engineering under Department of Mechanical Engineering of Jadavpur University., Kolkata – 700 032.*

Dr. Nabendu Ghosh
Assistant Professor
Department of Mechanical Engineering
Jadavpur University, Kolkata- 700 032

Mr. Abhishek Mandal
Assistant Professor
Department of Mechanical Engineering
Jadavpur University, Kolkata- 700 032

Dr. Swarnendu Sen
Professor and Head
Department of Mechanical Engineering
Jadavpur University, Kolkata- 700 032

Dr. Dipak Laha
Professor and Dean
Faculty of Engineering and Technology
Jadavpur University, Kolkata- 700 032

JADAVPUR UNIVERSITY

FACULTY OF ENGINEERING AND TECHNOLOGY

CERTIFICATE OF APPROVAL*

*The foregoing thesis entitled "**Synthesis and Parametric Optimization of Nickel-Cobalt-Phosphorus-Titanium Dioxide Electroless Coating**" is hereby approved as a credible study in the area of Production Technology, carried out and presented by Niladri Sekhar Dolui in a manner satisfactory to warrant its acceptance as a pre-requisite to the degree for which it has been submitted. It is understood that by this approval, the undersigned, do not necessarily endorse or approve any statement made, opinion expressed or conclusion drawn therein, but approve the thesis only for the purpose for which it has been submitted.*

Final Examination for Evaluation of the Thesis:

……. ……..

*Only in case this thesis recommendation is concurred in

ACKNOWLEDGEMENT

I take immense pleasure in expressing my deep respect, gratitude, and sincere appreciation to my esteemed thesis supervisors, Dr. Nabendu Ghosh and Abhishek Mandal, for their invaluable guidance, continuous inspiration, and genuine assistance throughout the entire duration of my project. Their contribution has not only nurtured my interest in the field but also served as a source of quiet inspiration through their intellectual prowess.

I am profoundly grateful to all the faculty members of Production specialization, Mechanical Engineering Department, as well as those in other disciplines, for their extensive cooperation during this endeavour.

Furthermore, I wish to convey my heartfelt thanks to the technical personnel at the Surface Engineering Lab, Metrology Lab, Metallography Lab, and Blue Earth Machine Shop at Jadavpur University. Their assistance in various technical aspects related to my research has been invaluable.

I wish to express my gratitude to Jadavpur University Research Scholar Mr. Biplab Baran Mandal, Mr. Vikash Kumar, Mr. Sovan Sahoo and Mr. Rupam Mandal for their unwavering academic support throughout the thesis. Their contributions were integral to the successful completion of the work.

The unwavering moral and financial support provided by my Mother and Brother played a crucial role in the successful completion of the thesis, without which it would have been an insurmountable task.

In conclusion, I extend my thanks to all individuals who have directly or indirectly supported me in completing this work.

Date- ……..

Jadavpur University Niladri Sekhar Dolui

Kolkata- 700 032

CONTENTS

Chapter 1: General Introduction

Chapter 2: Literature Review & Research Objectives

Chapter 3: Experimental Details

LIST OF FIGURES

LIST OF TABLES

Chapter 1:

Introduction

A coating, from a surface engineering point of view, is a layer of material deposited onto a substrate to enhance the surface properties for corrosion and wear protection. Factors affecting the choice of a coating include service environment, life expectancy, substrate material compatibility, component shape and size, and cost. There is a wide range of coating processes for depositing many different types of material at thicknesses ranging from just a few microns, up to several millimetres. The different types of coatings can be categorized in many ways. One common approach is based on the manner in which the coating material is deposited on the substrate surface. The history of coating spans thousands of years and encompasses a wide range of materials and techniques used to protect, preserve, and decorate surfaces. Here's an overview of the major developments in the history of coating:

Prehistoric Era: Early humans used natural substances like animal fats, waxes, and tree resins to coat tools and weapons for protection and durability.

Ancient Egypt: Egyptians used natural resins, gums, and waxes to coat and preserve mummies. They also applied gypsum and lime-based plasters to structures, sometimes adding pigments for decorative purposes.

Ancient China: The Chinese developed lacquerware as early as 3000 BCE, using the sap of the lacquer tree to create durable, glossy coatings for wooden objects and artworks.

Industrial Advancements: By the 18th century, innovations in chemistry led to the development of more advanced coatings. Linseed oil continued to be a primary binder, but new pigments and additives improved the durability and appearance of paints.

Industrial Revolution: The mass production of paints and coatings began, with the introduction of synthetic pigments and binders. The development of alkyd resins in the late 1800s provided more durable and flexible coatings.

Electroplating: Invented in the early 19th century, this technique allowed for the deposition of metal coatings (such as gold, silver, or nickel) onto surfaces for both decorative and protective purposes.

Synthetic Polymers: The development of synthetic polymers, such as acrylics, polyurethanes, and epoxies, revolutionized the coatings industry. These materials offered improved performance, durability, and versatility.

Automotive Industry: The automotive industry drove significant advancements in coatings technology, including the development of durable and aesthetically pleasing paints and the introduction of spray application techniques.

Environmental Concerns: The latter half of the 20th century saw a growing awareness of the environmental impact of coatings, leading to the development of water-based paints and low-VOC (volatile organic compound) formulations.

Nanotechnology: The application of nanotechnology in coatings has led to the development of materials with enhanced properties, such as scratch resistance, UV protection, and self-cleaning surfaces.

Sustainable Coatings: Ongoing research focuses on creating more sustainable and eco-friendly coatings, utilizing renewable resources and reducing the environmental footprint.

Smart Coatings: Innovations include smart coatings that can change color, self-heal, or provide other functionalities in response to environmental stimuli.

The history of coating reflects humanity's continuous effort to improve the durability, functionality, and aesthetics of materials, driven by advancements in technology and an evolving understanding of materials science.

1.1 Electroless Coating

The Electroless process is a self-sustaining technique where the conversion of metallic ions in the solution and the formation of a thin film can be achieved by the oxidation of a chemical compound found in the solution itself, specifically a reducing agent. This reducing agent is responsible for providing an internal electrical current. The process necessitates the reduction of a metal cation to be deposited by electrons received either from the surface of a metal substrate or from the catalysts utilized to kickstart the deposition process. Subsequently, the reductant transfers electrons to this surface, leading to its oxidation.

The electroless plating process involves the autocatalytic or chemical reduction of aqueous metal ions that are coated onto a base substrate without the need for an external current. This process specifically does not include methods like immersion plating, where metals are deposited without the use of current, such as copper deposited on steel immersed in a copper sulfate solution or nickel on steel immersed in a chloride and boric acid bath, and homogenous chemical

reduction processes like silvering. In galvanic displacement or immersion plating, the base material dissolves into the solution while metallic ions in the solution are concurrently reduced on the surface of the base material. This mechanism sets it apart from autocatalytic deposition, as in immersion plating, reducing agents are unnecessary to convert metal ions to metal since the base material itself acts as a reducing agent. Despite these distinctions, these methods have not been widely embraced due to their poor adherence and inferior properties. On the other hand, the electroless coating process has gained popularity in the market due to the exceptional corrosion and wear resistance properties of the coatings, making them suitable for soldering and brazing applications.

The disparity between the electroless plating process and immersion platingies in the fact that the metal deposition is achieved through an autocatalytic reduction process in the former, which does not necessitate the use of electrodes. Furthermore, it involves an autocatalytic reaction occurring on the metal surface post the initiation of nucleation. Conversely, an immersion plating solution functions based on the displacement of the substrate's surface skin by a more noble metal present in the solution. Despite being commonly categorized as electrochemical methods or electro-deposition processes, a clear distinction between electrolytic and electroless deposition processes is essential, as depicted in Fig. 1

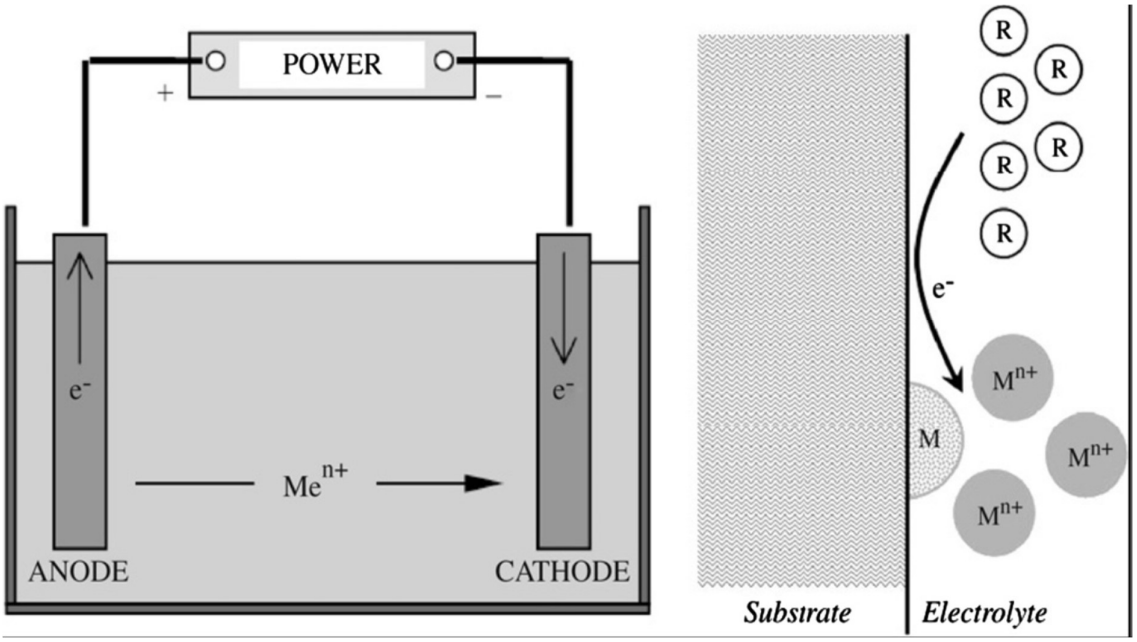

Fig. 1.1: Cell set up for (left side) electrolytic deposition process plus external power source; (right side) electroless deposition with reducing agent R as the source of electrons [31]

Advantages:

- Do not require electrical power.
- Electroless coatings provide uniform thickness and coverage, even on complex geometries and internal surfaces.
- Electroless coatings can coat irregular shapes and internal cavities without the need for masking or post-machining.
- Electroless coatings offer precise control over coating thickness, composition, and properties, allowing for tailored coatings with specific performance characteristics.
- No sophisticated jigs or fixture is required.
- There is flexibility in plating volume and thickness.
- Chemical replenishment can be monitored automatically.
- Complex filtration method is not required.
- Excellent corrosion resistance.
- Wear and abrasion resistance.
- Solder ability.
- High hardness.
- Both amorphous and microcrystalline deposit can be achieved.
- Low coefficient of friction.
- High reflectivity & Resistivity.
- Magnetic properties.

Disadvantages:

- Lifespan of chemicals is limited.
- Waste treatment cost is high due to the speedy chemical renewal.
- Electroless coating processes may require careful control of chemical parameters, temperature, and reaction time, which can increase process complexity and cost.

The electroless plating bath typically comprises a metal ion source, reducing agent, complexing agent, stabilizer, buffering agent, wetting agent, and parameters such as controlled temperature and pH. A summary of their functions can be found in **Table 1.** Electroless deposition is considered a sophisticated technique for applying alloy coatings, involving the autocatalytic reduction of cations at the interface of the substrate and solution through electrons provided by suitable reducing agents, resulting in the release of elements that allow for the co-deposition of reduced metals to create binary, ternary, or even quaternary alloys. The incorporation of composite materials in the alloy coating process leads to the formation of electroless composite coatings. Various metals such as nickel, copper, gold, silver, palladium, and

cobalt are commonly deposited using electroless plating. The industrial utilization of electroless nickel, particularly the nickel/phosphorus alloy, has experienced consistent growth in the past decade due to its unique properties. Although the autocatalytic deposition of nearly pure nickel utilizing hydrazine as the reducing agent has been established for some time, its industrial application remains limited. Nickel/phosphorus or boron alloys are predominantly associated with the term 'electroless' as 95% of industrial productions pertain to these alloys. Recently, electroless plating has garnered attention for its diverse applications in engineering, surface science, separation and purification technology, among others.

1.2 Historical overview of Electroless Coating

Electroless nickel is not a pure metal, but rather a composite material containing additional elements originating from the reducing agent, such as phosphorus or boron, and elements like thallium, lead, or cadmium obtained from supplementary bath additives. The progression in the early 1980s led to the discovery that phosphorus-rich depositions from an acidic bath exhibited superior wear and corrosion resistance compared to those formed under alkaline conditions, all achieved without the use of heavy metal stabilizers. These particular coatings exhibit a glassy, amorphous structure composed of extremely diminutive (5 nm) crystallites, while some are speculated to be genuinely amorphous, lacking any identifiable short-range order. Electroless nanocoatings are characterized by either the thickness of the coating or the integration of second-phase particles dispersed within the matrix at the nanoscale level. Electroless copper coating was initially employed prior to electroplating on non-conductive materials such as plastics, ceramics, and polymers, subsequently paving the way for other electroless metallic depositions. Since then, the field of electroless coating chemistry has emerged as a focal point in surface engineering and metal finishing research. General categories of the electroless nickel coatings are shown in Fig. 1.2.

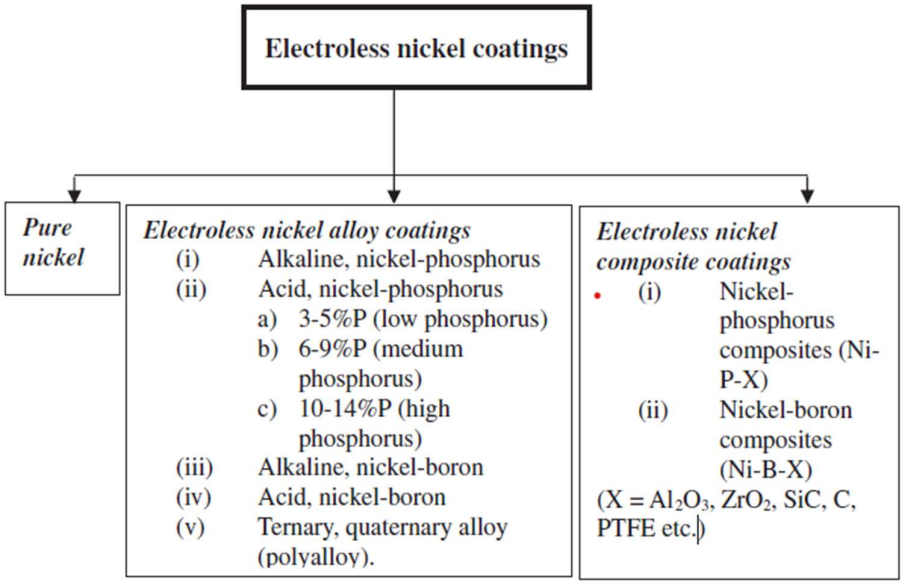

Fig. 1.2: General categories of electroless nickel coatings[31]

1.3 Basic principles of electroless plating

The fundamental requirement of an electroless bath involves the presence of metal ions and their concentration, as well as the inclusion of reducing agents, complexing agents, bath stabilizers, and the regulation of pH and temperature. Within the realm of electroless deposition, metal ions undergo a reduction to metal through the influence of chemical reducing agents, which function as electron donors. These metal ions, serving as electron acceptors, engage in reactions with the electron donors. This process is characterized as autocatalytic, thereby expediting the electroless chemical reaction and enabling the oxidation of the reducing agent utilized. The schematic representation in Fig. 1.3 illustrates the standard apparatus typically employed in electroless experiments.

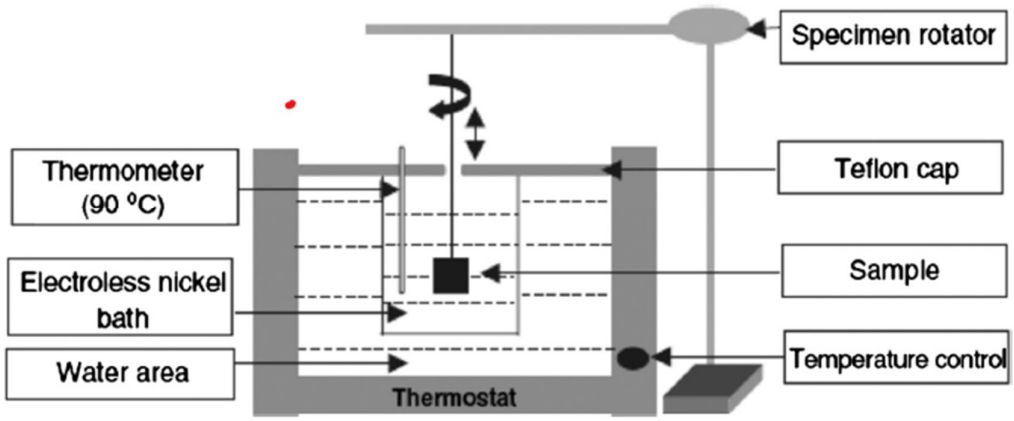

Fig. 1.3: Basic diagram of the apparatus usually used in electroless experiments. [31]

1.3.1 Reducing Agent

Numerous reducing agents have been introduced into the commercial market, such as sodium hypophosphite, amino boranes, sodium borohydride, and hydrazine (refer to Table 1.1).

1.3.2 Sodium hypophosphite baths

Electroless deposition using a hypophosphite bath offers advantages compared to baths utilizing boron and hydrazine reductions. The hypophosphite bath is more cost-effective and provides superior corrosion resistance. The process of reducing metal ions with hypophosphite involves two distinct reactions: the catalytic oxidation of hypophosphite ions and the reduction of nickel ions at the catalytic surface. A portion of the hydrogen released is absorbed onto the catalytic surface, constituting an anodic reaction. Subsequently, the nickel ion on the catalyst's surface is reduced by the absorbed active hydrogen, representing a cathodic reaction. Electroless nickel coatings have gained significant commercial importance and are extensively discussed in various contexts.

Electroless bath	Pure nickel	Acid nickel–P/B	Alkaline nickel–P/B
pH	10.5–11	4.5–5.5 Medium and high P/B; 6.0–6.5 low P/B	8.5–14
Temperature (°C)	85–90	75–95	25–95
Deposition rate (μm/h)	6–12	10–25	10–15
Metal salts or source	Nickel acetate	Nickel sulfate, nickel chloride	Nickel sulfate, nickel chloride
Reducing agents	Hydrazine	Sodium hypophosphite, sodium borohydride, dimethylamine (DMAB)	Sodium hypophosphite, sodium borohydride, dimethylamine (DMAB), hydrazine
Complexing agents	EDTA (tetra sodium salt), glycolic acid	Citric, lactic, glycolic, proprionic acids, sodium citrate, succinic acid	Citric, lactic, glycolic, proprionic acids, sodium citrate, sodium acetate, sodium pyrophosphate
Stabilizers		Thiourea, lead acetate, heavy metal salts, thioorganic	Thiourea, lead acetate, heavy metal salts, thioorganic compound, thallium, selenium
pH adjusters		Sodium hydroxide, sulfuric acid	Sodium hydroxide, sulfuric acid, ammonium hydroxide

Table 1.1: Typical components, operating conditions and applications of different electroless nickel coating baths.[31]

1.3.3 Amino boranes baths

Two varieties of aminoboranes are currently utilized in the commercial sector, specifically N-dimethylamine borane (DMAB) and N-diethyalmine borane (DEAB). These substances exhibit notable efficacy as reducing agents across a broader spectrum of pH levels in comparison to borohydrides. Nickel solutions containing amino boranes are operational within both acidic and alkaline environments. The resultant reduction reactions yield both metallic nickel and nickel boride. Typically, the conversion of 1 kg of dimethylamine borane is necessary for the reduction of 1 kg of nickel. Amine boranes serve as proficient reducing agents for the electroplating of plastics, non-metals, and are also instrumental in the electroless deposition of various metals like copper, gold, silver, and cobalt.

1.3.4 Sodium borohydride baths

Sodium borohydride represents the most potent reducing agent accessible for electroless nickel plating. Within the acidic and neutral pH spectrums, borohydrides undergo swift hydrolysis, leading to the formation of nickel boride in the presence of nickel ions. Conversely, in alkaline solutions with a pH exceeding 13, borohydride experiences catalytic decomposition. Consequently, nickel boride is generated in the presence of nickel ions. Typically, 600 grams of sodium borohydride are necessary for the reduction of 1 kilogram of nickel, resulting in nickel deposits with a purity exceeding 92.97%. The occurrence of spontaneous solution decomposition is plausible if the pH of the bath decreases below 12. Due to the elevated operational pH levels, borohydride plating baths are unsuitable for application on aluminum substrates.

1.3.5 Hydrazine bath

Hydrazine solution has been employed for the generation of high-purity electroless nickel coating (99% purity). Due to its susceptibility to decomposition under elevated temperatures, these solutions manifest a notable propensity for instability and pose challenges in terms of regulation. Further elaboration on the intricacies of the pure nickel segment will be provided.

1.3.6 Complexing agent

Complexing agents are incorporated for the purpose of preventing the degradation of solutions and regulating the reaction in such a manner that it

exclusively takes place on the catalytic surface. These agents, which are organic acids or their corresponding salts, are introduced to manage the quantity of available free electron (nickel) for the reaction. Furthermore, the inclusion of complexing agents aids in buffering the solution and impeding the precipitation of nickel phosphite. Additionally, ammonia, hydroxides, or carbonates might need to be intermittently introduced to counteract the presence of hydrogen. The utilization of a complexing agent in the electroplating solution can also impact the quality of the deposition, particularly in terms of phosphorus content, internal stress, and porosity.

1.3.7 Accelerator

Accelerators are frequently introduced into the electroplating solution in small quantities to enhance the deposition rate, leading to a potentially significant increase in plating efficiency. The primary role of an accelerator is to disrupt the bond formation between hydrogen and phosphorus atoms within the hypophosphite molecule, facilitating the easier removal and absorption of phosphorus onto the catalytic surface. Although succinic acid is not explicitly mentioned in Table 2 for hypophosphite-reduced solutions, it is commonly utilized as an accelerator.

1.3.8 Inhibitor and by-products

The incorporation of inhibitors, also known as stabilizers, outlined in Table 2, may yield both advantageous and detrimental outcomes on the plating solution and its resultant coating. Certain inhibitors, when present in minimal quantities, can accelerate the deposition rate and enhance the luster of the coating. The substrate ought to possess catalytic properties; in cases where it does not, the surface must undergo appropriate catalytic treatment prior to immersion in the electroless solution, initiating a uniform deposition process. Once the deposition occurs, the substrate functions as a catalyst, perpetuating the process. Throughout the electroless nickel deposition, side products of the reduction process, such as orthophosphate or borate, hydrogen ions, and dissolved metal from the substrate, accumulate within the solution. These side products influence the deposition rate of the solution and marginally elevate the phosphorus/boron content of the coating. Elevated levels of orthophosphate in the plating solution can lead to rough coatings and spontaneous decomposition of the solution. Parameters such as temperature, pH, metal ion concentration, and the level of reducing agent dictate the rate of coating application.

1.4 Electroless Nickel Coating

Electroless nickel plating is widely embraced in engineering applications due to its distinctive characteristics, which encompass outstanding resistance to corrosion, wear, and abrasion, as well as ductility, lubrication, soldering, and electrical properties. These coatings exhibit a more consistent thickness compared to electroplated nickel coatings. The plating solutions utilized for electroless Ni primarily consist of nickel sulfate (Ni source), sodium hypophosphite (reducing agent), and additives to hinder the precipitation of insoluble nickel hydroxide. Operating at approximately 85 C, the baths maintain an acidic pH range for stability, yet the pH can decrease due to hydrogen evolution; to counteract this, alkaline salts of Na and K or ammonium ions are typically introduced. The coulometric method demonstrates sensitivity towards fluctuations in phosphorus levels within the coating. On the other hand, the magnetic method is responsive to variations in the coating's permeability. Similarly, the eddy current method is sensitive to changes in both phosphorus content and permeability of the coating.[31]

Electroless nickel coatings may consist of four major types, as follows:

(1) Pure nickel and black nickel coatings.
(2) Electroless nickel alloy coatings.
    Acid bath: Ni–P alloy, 3–5% P (L), 6–9% P (M), 10–14% P (H).
    Alkaline bath: Ni–P alloy.
    Acid bath: Ni–B alloy, 0.1–2% B (L), 2–5% B (M), 5–10% B (H).
    Alkaline bath: Ni–B alloy.
    Poly-alloys.
(3) Electroless composite coatings.
(4) Electroless nano-coatings.

1.4.1.1 Pure Nickel

The utilization of phosphorus/boron alloy in conjunction with nickel has been observed due to their distinct characteristics in contrast to electrodeposited Watts nickel. Nevertheless, a 'pure' autocatalytic nickel could prove highly beneficial for specific applications, particularly in the realm of semiconductor applications. This transformation is commonly facilitated by the application of hydrazine. The standard composition of the bath consists of 60 g/l nickel acetate, 60 g/l glycolic acid, 25 g/l EDTA (tetrasodium salt), 100 g/l hydrazine, and 30 g/l sodium hydroxide. The operational parameters encompass a pH range of 10.5-11, a temperature range of 85-90°C, resulting in a deposition rate of 6-12 μm/h. The initial hardness of the as-deposited pure nickel coating is

measured at 450 HV. Subsequent to a heat treatment at 450°C for 1 hour, the coating exhibits a significant decrease in hardness to 125 HV, accompanied by a substantial enhancement in ductility.

1.4.1.2 Black Nickel

It is feasible to acquire it from both electro and electroless deposition surfaces through the process of surface etching using oxidizing acidic solutions [42]. The electroless nickel deposit, due to its phosphorus content, can be easily etched by oxidizing acids to achieve an ultra-black surface. Blackening of the electroless nickel deposit occurs by immersion in a nitric acid solution with a concentration of (9 M). The initial appearance of blackening, resulting from hole formation, is observed at the boundaries between different nodules and eventually spreads across the entire deposit surface on titanium alloy . This specific structure, generated through selective etching, effectively traps light and exhibits the capability to absorb over 99% of light in the solar region (0.3–2 μm) . Furthermore, these surfaces are highly effective in enhancing the absorption capabilities of thermal detectors and in reducing the impact of stray and scattered light in optical instruments and sensors. To achieve optimal ultra-high optical properties for blackening, an electroless nickel thickness of 35 ± 5 μm is deemed necessary. Electroless nickel coatings containing 7% phosphorus are suitable for further blackening processes. Alloys with higher phosphorus content are unsuitable due to their excessive corrosion resistance, hindering the blackening effect of acid etching. The primary constituents of the black coating are identified to comprise NiO, Ni2O3, and some nickel phosphate. The blackened electroless nickel demonstrates superior optical properties with a solar absorbance of 0.85as; this coating exhibits excellent adhesion, uniformity, and stability even under harsh space conditions. Consequently, it finds extensive application as a solar absorber in solar-related technologies.

1.4.2 Electroless nickel alloy coating

1.4.2.1 Acid bath Ni–P alloy

The advantages of hot acid solutions over alkaline solutions have been well-documented in the literature. Hot acid electroless nickel baths are predominantly utilized for the deposition of thick coatings on metal substrates. The quality of the coatings derived from acid solutions is superior, and the

stability of the bath solution during plating is notably enhanced. It is important to note that the thermal stability, particularly upon heating and crystallization, should not be reliant on the solution composition. The control of phosphorus content is easily achievable while considering the unique properties of these solutions. These coatings can be categorized into three groups:

- Low phosphorus content of 3-5%, known for their outstanding wear resistance and corrosion protection against concentrated caustic soda;
- Medium phosphorus content of 6-9%, offering adequate corrosion protection and abrasion resistance for various applications; and
- High phosphorus content of 10-14%, characterized by high ductility and corrosion resistance, especially against chlorides and mechanical stress.

1.4.2.2 Alkaline bath Ni–P alloy

Hot nickel-phosphorus deposits in an alkaline environment are commonly reduced using sodium hypophosphite. A typical solution consists of 30 g/l nickel chloride, 10 g/l sodium hypophosphite, 65 g/l ammonium citrate, and 50 g/l ammonium chloride. Operational parameters include a pH range of 8–10, a temperature range of 80–90°C, resulting in a deposition rate of 10 μm/h. The primary drawback of this alkaline solution is its high instability at temperatures exceeding 90°C, leading to a sudden decrease in bath pH due to ammonia loss. On the positive side, the alkaline low-temperature bath offers a convenient method for nickel deposition on plastics. Another common bath composition comprises 20 g/l nickel chloride, 24 g/l sodium hypophosphite, 45 g/l sodium citrate, and 30 g/l ammonium chloride. Under operational conditions of pH 8–9 and a temperature range of 30–40°C, a deposition rate of 8 μm/h is achieved. These deposits exhibit good solderability for the electronics industry. However, limitations include lower corrosion resistance, weaker adhesion to steel, and challenges in processing aluminum due to elevated pH levels.[31]

1.4.2.3 Acid bath Ni–B alloy

DMAB is commonly utilized as a reducing agent in acidic baths for the deposition of electroless nickel–boron coatings with boron concentrations ranging from 0.1% to 4%. The primary benefit of employing the hot acidic bath lies in its robustness, leading to coatings with a remarkably high melting point of 1350 C. These coatings find extensive use in industrial settings due to their inherent hardness upon plating, surpassing that of nickel–phosphorus.

Moreover, they exhibit favorable characteristics for soldering, brazing, and ultrasonic bonding when the boron content exceeds 1%. Typically, the reduction of boron is achieved through alkyl amine, with a potential to reach up to 5% through the use of specific accelerators. A standard bath composition consists of 30 g/l nickel chloride, 3 g/l diethylamine borane, 40 g/l methanol, 4 g/l dimethylamine borane (DMAB), 20 g/l sodium acetate, 20 g/l sodium succinate, and 10 g/l sodium citrate. The operational parameters entail maintaining a pH range of 5–6, a temperature of 50–60 C, resulting in a deposition rate of 15–20 μm/h. [31]

1.4.2.4 Alkaline bath Ni–B alloy

The primary benefits of nickel deposits reduced by borohydride include their notable hardness and exceptional resistance to wear in their original state. Dervos et al. introduced a method of vacuum heating that achieves surface hardness levels typically requiring lengthy conventional procedures in a significantly shorter timeframe, specifically less than 30 minutes, compared to heating in an inert atmosphere. Through a 5-minute thermal process conducted in a high vacuum setting, a surface microhardness equivalent to chromium is attained, locally reaching up to 2000 HV in certain instances, all without the harmful environmental effects associated with hard chromium plating. This technique is applicable across various industries seeking alternatives to hard chromium plating. Kanta et al. examined nickel-boron coatings on mild steel, subjecting them to diverse post-treatments such as heat-treatments in a 95% Ar and 5% H2 environment at 400°C for an hour, as well as thermo-chemical treatments. The latter involved a process in a nitrogen-rich atmosphere at 500°C for two hours, followed by an ammonia-based treatment. Upon undergoing heat and thermo-chemical treatments, nickel-boron coatings crystallize and yield nickel alongside nickel borides within the coatings. These authors also applied the Ni-P and Ni-B system on steel and specially prepared aluminum substrates, the latter safeguarded by an outer Ni-P layer, resulting in a smoother surface and exhibiting a more noble electrochemical behavior compared to Ni-B. Furthermore, nanocrystalline nickel-boron deposits were synthesized on mild steel substrates to improve the mechanical and wear-resistant properties of the coatings. [31]

1.4.2.5 Poly-alloy

The electroless process is considered a sophisticated technique for the deposition of alloy coatings. In academic literature, ternary and quaternary alloys are commonly known as polyalloys. Notably, alloys such as Ni–Co–P, Ni–Fe–P, and Ni–Co–Fe–P have gained significant usage due to their exceptional magnetic characteristics. Films with high coercivity are utilized in

high-density recording applications, while low-coercivity alloys are recommended for high-speed computing purposes. A ternary alloy like Ni–Cu–P (with 1 at.% Cu) displays notable corrosion resistance and ductility compared to standard Ni–P alloy. Another ternary alloy, Ni–Mo–B, containing molybdenum, exhibits good solderability and is particularly advantageous in the electronics industry due to its non-ferromagnetic properties. The incorporation of tungsten in ternary alloys enhances hardness and corrosion resistance, with tin-containing alloys up to 40% being recognized for their corrosion resistance. Polyalloys are typically applied in scenarios requiring specific chemical, high-temperature, electrical, magnetic, or non-magnetic properties. The selection of alloy coatings is based on intended applications and economic factors. A comprehensive overview of electroless deposited alloy features and non-electrolytic metallic alloy coatings. The addition of a third element in electroless Ni–P plating significantly impacts the properties of the coatings. Introducing Cu or Sn in electroless Ni–P improves thermal stability, preserves paramagnetic behavior, and enhances corrosion resistance. Notably, a Cu content of 17.2 wt.% in Ni–Cu–P coatings demonstrates superior anti-corrosion performance. The presence of Cu in Ni–Cu–P coatings promotes selective dissolution of Ni, leading to the enrichment of P and Cu on the surface layer, thereby enhancing corrosion resistance. These coatings are utilized in practical flue gas condensation and show promise for heat exchanger applications. Additionally, hybrid multilayer deposits like Ni–Cu–P/Ti/TiN on mild steel exhibit improved mechanical properties such as friction coefficient and nano-hardness compared to single-layer Ni–Cu–P coatings, suggesting potential for enhanced corrosion resistance and mechanical behavior.

1.5 Ni-P Electroless coating Properties

1.5.1 Physical properties

1.5.1.1 Deposit uniformity

This particular physical characteristic represents a crucial aspect and a notable benefit of the electroless nickel technique. It pertains to the capacity for achieving consistent thickness on components featuring intricate geometries and forms. The influence of current density commonly observed in electroplating processes is irrelevant in this context, allowing for the uniform plating of sharp edges, intricate grooves, and enclosed cavities with electroless nickel. Electrode positioning may result in excessive material buildup at raised areas and edges, necessitating finishing through grinding. These issues are circumvented by electroless depositions**.**

1.5.1.2 Structure

The amalgamations comprise a blend of disordered and minute crystalline nickel at modest and intermediate phosphorus levels, transitioning to a fully disordered state with elevated phosphorus content. Subsequent to exposure to 800°C, the resultant depositions consist entirely of Ni3P and stable f.c.c. nickel phases. Transitional metastable phases like NiP2 an might emerge with elevated phosphorus levels prior to the establishment of the stable Ni3P phase. Alterations in the structure of Ni-P commence at temperatures surpassing 220–260°C, leading to the crystallization and loss of the disordered structure in the deposition. The inception of nickel phosphite (Ni3P) transpires within the alloy once the temperature surpasses 320°C, achieving optimal crystalline structure subsequent to heating at 400°C for an hour, yielding heightened corrosion resistance, hardness, and wear resistance. Coatings with over 9% phosphorus content develop a nickel phosphite (Ni3P) matrix, while deposits with lower phosphorus content are predominantly composed of pure nickel. To prevent the occurrence of the blue hue in the thermally treated specimens resulting from the amalgamation of the oxide layer with oxygen, it is imperative to seclude them within a vacuum furnace. Heat-treated samples exhibit enhanced hardness and wear resistance, albeit at the expense of reduced corrosion resistance. In the case of Ni–B, the typical coating encompasses 5% boron and in contrast to Ni–P, Ni–B comprises a mix of crystalline nickel intertwined with a nickel–boron (Ni2B) vitreous structure.

1.5.1.3 Density

The density of electroless Ni-P and Ni-B exhibits similarity to that of alloys with equivalent content. Such similarity demonstrates an inverse relationship with the phosphorus/boron content as indicated in previous studies [85,86]. Within this context, the density is observed to fluctuate within the range of 8.5 gm/cm3 (low P) to 7.75 gm/cm3 (high P), while remaining at 8.25 gm/cm3 for compositions containing 5% B.

1.5.1.4 Melting point

The electroless Ni–P deposits exhibit a melting range rather than a specific melting point, contrasting with electrolytically deposited nickel. Pure nickel typically melts at 1455°C; however, an increase in phosphorus content causes the deposit to undergo softening at lower temperatures. Deposits of Electroless Ni–P with 11% P display a minimum melting point of 880°C. Those with low phosphorus concentrations (below 3%) demonstrate the highest melting points, approximately around 1200°C. In comparison, Ni–B possesses a relatively elevated melting point. Electroless Ni–B deposits reduced by sodium

borohydride and containing 5% B exhibit a melting point of 1080°C, while in a bath reduced by DMAB, the melting point ranges from 1350 to 1360°C.

1.5.1.5 Electrical resistivity

The electrical resistivity of electroless nickel alloys is higher than that of pure nickel [87]. Pure nickel exhibits a specific resistivity of 7.8 x 10^6 ohm cm. An increase in phosphorus content leads to a corresponding rise in electrical resistivity, with values ranging from 30 to 100 x 10^6 ohm cm depending on the deposition conditions. Conductivity of electroless Ni-P can be enhanced through heat treatment, influencing its resistivity. In the as-deposited state, the electrical resistivity of 9% phosphorus is 89 x 10^6 ohm cm and decreases to 43 x 10^6 ohm cm after heat treatment at 1100°C. The resistivity characteristics of Ni-B are comparable to those of Ni-P, with a resistivity value of 89 x 10^6 ohm cm for 5% boron. Ni-B finds significant applications in electronic industries due to its low resistivity properties.

1.5.2 Mechanical properties

The mechanical characteristics of the deposit are primarily influenced by the concentration of phosphorus and boron. Typically, the coatings exhibit elevated strength levels, restricted ductility, and a high elastic modulus. Commercial coatings possess an ultimate tensile strength surpassing 700 MPa, enabling them to endure loading conditions without succumbing to damage

1.5.2.1 Internal stress

The primary function of coating composition lies in the internal stress within electroless nickel coatings. Tensile stresses ranging from 15–45 MPa emerge in deposits with lower phosphorus content due to thermal expansion variations between the deposits and the substrate. Cracking and porosity are promoted in these coatings by the significant stress levels present. When subjected to heat treatment exceeding 220°C, structural modifications lead to a volumetric contraction of electroless nickel deposits by as much as 6%, consequently enhancing tensile stress and diminishing compressive stress in the coating. The addition of orthophosphites or heavy metals during deposition, along with the surplus of complexing agents in the plating solution, can further elevate deposit stress. Even minute quantities of certain metals can significantly escalate stress levels. Furthermore, heightened internal stress levels diminish the ductility of the coating.

1.5.2.2 Ductility

The ductility of the electroless Ni–P coating exhibits variation according to its composition. The incorporation of composites during deposition process has an impact on the ductility characteristics. When the deposits have a relatively high phosphorus content in the as-deposited condition, they demonstrate a ductility range of 1–1.5% (in terms of elongation). Despite being less ductile compared to the majority of engineering materials, this level of ductility is deemed suitable for various coating applications. In fact, thin layers of the deposit can be bent fully around themselves without experiencing any fractures. Conversely, a decrease in phosphorus content leads to a significant reduction in ductility, potentially approaching zero. The ductility of electroless Ni–B is approximately one-fifth (0.2%) of that observed in high phosphorus deposits. Nonetheless, the influence of heat treatment on ductility is minimal.

1.5.2.3 Tensile strength

The tensile strength of Ni–P deposits surpasses that of Ni–B deposits. In the as-deposited state, a low phosphorus deposit exhibits a tensile strength ranging from 450 to 550 MPa. Ni–P deposits that have undergone heat treatment demonstrate reduced tensile strength compared to the as-deposited ones, yet their hardness is enhanced. This reduction is identified to be within the range of 200–300 MPa.

1.5.2.4 Hardness

The hardness of electroless Ni–P and Ni–B coatings in the as-deposited state is comparable to that of numerous hardened alloy steels. This stands in contrast to electrolytically deposited nickel in the as-deposited state, which typically exhibits hardness values ranging from 150 to 400 HV0.1. Through heat treatment, EN coatings can achieve hardness levels similar to those of electrodeposited chromium. Optimum hardness is reached within 1 hour at approximately 400°C or within 10 hours at 260°C. The capacity of electroless nickel deposits to retain their hardness in elevated-temperature operating conditions improves with higher phosphorus or boron content, although it diminishes significantly beyond 385°C. Ni–B coatings demonstrate superior resistance to wear at elevated temperatures, making them a preferred choice for such environments. offers a comparison of the hardness of electroless nickel coatings in the as-deposited and heat-treated states based on phosphorus/boron content. Yan et al. succeeded in achieving a high hardness value of 910 HV0.1 for as-deposited Ni–P coating with an 8 at.% phosphorus content by adjusting the ratio of lactic acid to acetic acid in the electroless bath, consequently enhancing wear resistance.

1.5.2.5 Solderability

Electroless nickel–phosphorus is more readily solderable in comparison to boron deposits, particularly in electronic applications for enhancing the soldering process of lightweight metals like aluminum. The commonly used combination involves Rosin mildly activated (RMA) flux with traditional Sn–Pd solder. Elevating the component's temperature to around 100 degrees Celsius prior to soldering enhances the efficiency and speed of the joining process, with the flux primarily serving the purpose of wetting the coated surface.

1.5.2.6 Frictional properties

These parameters also differ depending on the phosphorus/boron levels and the specific heat treatment processes employed. They exhibit similarities to the properties of chromium. The presence of phosphorus contributes to inherent lubricating properties, particularly advantageous in scenarios such as plastic molding applications. When comparing the frictional characteristics between electroless nickel/boron and steel, the coefficient ranges from 0.12 to 0.13 under lubricated conditions and 0.43 to 0.44 without lubrication.

1.6 Electroless Nickel composite coatings

The co-deposition of composite materials (hard particle or nonmetallic) with electroless coatings is referred to as electroless composite coatings. The production of wear-resistant composite is achievable through the co-deposition of fine particulate matter. Various hard particles like diamond, silicon carbide, aluminum oxide, as well as solid lubricants such as polytetrafluoroethylene (PTFE) particles, have been jointly deposited. Additional small particles of intermetallic compounds and fluorocarbons can be dispersed within an electroless nickel–phosphorus/boron matrix. Initially, electroless composite coatings faced challenges and often led to the decomposition of the bath. This issue arises from the dispersion of fine particles which significantly increases the surface area loading of the electroless bath, making it approximately 700–800 times more than that of a normal electroless bath, thus causing bath instability. However, with the assistance of suitable stabilizers, electroless nickel composite coating was successfully developed. In contrast to electro co-deposition, electroless coating enables the precise reproduction of surfaces while avoiding subsequent mechanical finishing.

Particle sizes range from sub-micron alumina and PTFE to 5-μm diamonds. To ensure better integration between particles and the electroless nickel-phosphorus matrix, it is imperative for particle sizes to be small enough to be securely held

by the matrix. Research by Apachitei et al. revealed that spherical Al2O3 particles exhibited superior incorporation compared to irregular ones. The shape of particles also influences the final deposit finish, with large angular particles resulting in very rough surfaces and small rounded particles yielding very smooth surfaces. Various particles such as silicon carbide (SiC), chromium carbide (CrC), zirconia or aluminum oxide (ZrO2, Al2O3), graphite, and PTFE have been investigated by multiple researchers. The critical requirements of electroless nickel composite coating are succinctly summarized below.

- The stability of the bath is influenced by the dispersion of fine particles, which in turn increases the surface area loading and contributes to the decomposition of the bath.
- Agitation is a crucial aspect to consider. For instance, hard particles like diamond, silicon carbide, and aluminum oxide are effectively maintained in suspension through agitation, leading to their occlusion in the deposit. It is advisable to rotate and/or tumble objects in a manner that ensures all surface areas are consistently exposed upwards. The agitation of the plating solution stands out as a key determinant in this process
- The size of particles holds significant importance. Particles of appropriate shape and size need to be insoluble in the solution, devoid of surface contaminants, and maintained in suspension within the bath. The size of the particles significantly impacts the quality of the deposit.
- The concentration of particles is a critical factor to consider. At concentrations beyond a certain threshold, there is a risk of agglomeration among these secondary phase particles due to a reduction in the average distance between them, ultimately leading to particle settling. This settling process can result in either saturation or a slight decline in the level of incorporation. Therefore, the concentration plays a pivotal role in the even distribution of particles within the deposit.
- Surface-active agents, known as surfactants, are of particular significance in facilitating the introduction of pliable particles such as polytetrafluoroethylene (PTFE), graphite, and molybdenum disulfide. Their involvement is crucial in the integration of secondary phase particles as well.

The concentration of the dispersed particles in the electroless nickel bath is highlighted as a significant factor influencing the level of incorporation, as previously stated. Each composite material exhibits unique characteristics. A volume percentage of 20-25% SiC has demonstrated the highest hardness, surpassing that of Ni-P alloy coatings. Similarly, a volume percentage of 20-25% PTFE has been proven to decrease friction among engineering components that are plated with it. These composites are widely used in commercial applications, especially when there is a need for enhanced wear resistance or a

low coefficient of friction. While graphite presents itself as an alternative to PTFE, it is worth noting that PTFE enjoys robust industrial utilization.

Sodium dodecyl sulfate (SDS) is employed to enhance the dispersion and wettability of the SiC particles. Grosjean et al. demonstrated that the introduction of Forafac-500 led to an increase in the co-deposition of SiC particles from 19 to 53 vol.% [115]. Ger and Hwang postulated that the addition of surfactants facilitated a higher degree of integration of PTFE particles, with a crucial emphasis on their concentration within the solution. The variation in composition of the coating is intricately linked to the cathodic reactivity of the surfactants, particularly based on the substrates during the initial stages. Higher cathodic reactivity of the surfactants corresponds to easier embedding of PTFE particles in the co-deposition layer. The proportion of PTFE loading increases as the co-deposition coating expands, provided that the cathodic reactivity of surfactants on a substrate is lower compared to that on the deposited layer. Elevating the volume fraction of PTFE loading as the co-deposition layer grows fosters strong adhesion between the substrate and co-deposition layers. Recent research indicated that the incorporation of PTFE, along with appropriate types and concentrations of surfactants, results in uniform distribution of PTFE particles within the Ni–P matrix. CTAB and polyvinylpyrrolidone (PVP) promote even distribution of PTFE particles in the coating, while SDS does not achieve this outcome. A comprehensive comprehension of the impact of process parameters and conditions on electroless nickel deposits, as well as the characteristic properties of the second phase particles utilized for integration, represents a fundamental initial phase towards achieving successful composite integration.

The proportion by weight of hard and soft particles co-deposited within the electroless Ni–P/B can be quantified through the dissolution of a specified mass of the deposit in nitric acid followed by filtration of the particles using a 0.1 μm membrane that has been pre-weighed. Various alternative techniques have been suggested for evaluating the level of inclusion of secondary phase particles in electroless nickel–phosphorus/boron matrices. For instance, the incorporation of Cr_3C_2 can be assessed using an electron microprobe analyzer (EPMA), while the examination of the coating's cross-section through image analysis, as proposed by Bozzini et al. and also employed by Pena-Munoz et al. and Straffelini et al., is another approach. Yu and Zhang introduced the use of a plasma emitting spectrum analyzer, which enables direct identification of the constituents within the coating. Furthermore, Łosiewicz et al. utilized a method involving particle counting based on the observation of the surface morphology of EN-TiO2/PTFE coatings. These methodologies offer valuable means for determining the incorporation of particles in electroless composite coatings.

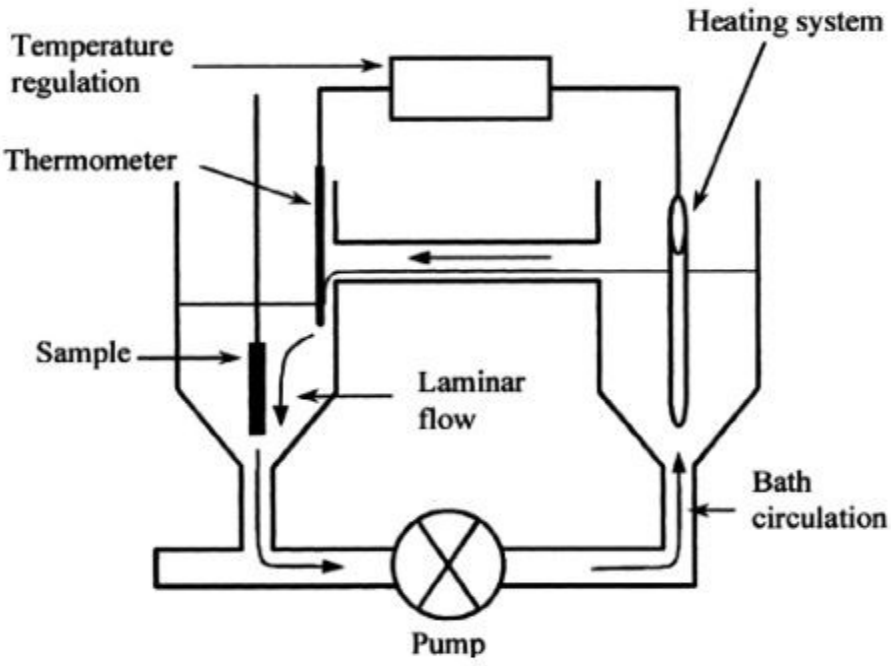

Fig 1.4: Experimental set-up recommended for producing electroless composite coatings [31]

1.6.1 Structure

The incorporation of Si_3N_4, CeO_2, and TiO_2 particles within the electroless Ni–P matrix deposit does not alter its structural composition as reported in reference. On the other hand, the introduction of B4C particles has been observed to impact the orientation of nickel crystallites while not affecting their dimensions. Specifically, it leads to a reduced orientation of nickel in layers containing B_4C particles, as documented in reference. Researchers Balaraju and Rajam noted in their studythat the presence of Si3N4 particles in the electroless Ni–P matrix does not bring about any significant changes in the structure of the composite coating. However, Apachitei et al. observed the reflection of SiC in the XRD pattern of the as-deposited electroless Ni–P–SiC composite coating, attributing it to a higher co-deposition of particles at 7 wt.%, as mentioned in reference. In a separate study, Jiaqiang et al. investigated the integration of SiCparticles into the electroless Ni–P matrix, resulting in the crystallization of nickel crystal, nickel phosphide, and nickel silicides post heat treatment at 400°C for 1 hour. Subsequent heat treatment at 600°C did not reveal any distinct diffraction peak corresponding to nickel silicides, except for Ni3Si, whose lattice closely resembles that of nickel, as reported in reference. The final outcomes of the crystallization and reaction processes in composite coatings included the formation of Ni, Ni_3P, Ni_3Si, and free carbon.

1.6.2. Hardness

These composite coatings are purported to exhibit significantly enhanced hardness properties for tools utilized at room temperatures, including molds, plastic extruders, metal patterns, core boxes for castings, forging dies, and zinc alloy casting dies. The hardness of these coatings is influenced by the quantity of co-deposition particles, the phosphorus content of the matrix, and the heat treatment process. A rise in the number of hard particles (e.g., SiC, Si3N4) in the coating results in an increase in hardness, while the presence of soft particles (e.g., PTFE) leads to a decrease in hardness. Notably, hard particles are the key factor contributing to hardness improvement across all phosphorus contents (2–14 wt.% P). The impact of heat treatment on the hardness of composite coatings follows a similar pattern to that observed in plain electroless Ni–P deposits. The increase in hardness up to 400°C is attributed to precipitation hardening through the formation of the intermetallic Ni3P phase. However, hardness diminishes beyond 400°C due to a reduction in lattice defects and the coarsening of Ni3P particles. Research by Dong et al. highlighted the substantial enhancement in mechanical properties of electroless Ni–P coatings achieved by incorporating SiO2 nanoparticles, resulting in a significant increase in microhardness (after treatment at 400°C) and wear resistance. Another study by Chen et al. introduced a novel Ni–P–TiO_2 composite coating method by integrating transparent TiO2 sol into the traditional electroless plating solution. As a result, microhardness saw a considerable enhancement from 710 $HV_{0.2}$ in the conventional Ni–P–TiO_2 coating to 1025 $HV_{0.2}$. Comparatively, the Ni–Zn–P–TiO_2 composite coatings exhibited superior microhardness compared to pure Ni–Zn–P alloy.

1.6.3 Applications

The primary utilization of electroless composite coatings pertains to machining and finishing tools that necessitate optimal wear resistance, surface friction coefficient, and a hard surface. The utilizations are delineated below. Ni–P–SiC (50 μm thick) enhances the longevity of molds utilized in plastics, rubber, etc., by a factor of 15. It serves to shield against the hastened corrosion of abrasion molds in the plastic sector (exceeding chrome plating), and is applicable in automotive components like reinforced plastic front-end pieces, as well as in foundries to diminish wear and aid in the extraction of sand cores from core boxes without breakage. Ni–P–PTFE provides non-adhesive, non-scuffing, high dry-lubrication, low friction, commendable wear and corrosion-resistant surfaces. It is employed in molds for rubber and plastic elements, pumps and valves, butterfly valves for the oil and gas domain, fasteners, precision instrument parts, aluminum air cylinders, carburetor and choke shafts. It reduces the leakage rate and facilitates the secure operation of the valve for cryogenic

applications. Dry lubrication and a low coefficient of friction are evident in the accumulation of sticky residues on the choke shafts. Other applications encompass chains, lock components, valves, pistons, piston rings, roller bearings, components of mining equipment, and dies. Ni–P–C is administered to reamers crafted from highly abrasive aluminum alloys, broaching tools for graphite, valves for viscous rubber compounds, thread guides utilized in textile machinery and friction texturizing discs, slip-free transmission of high rotational speeds, yarn brakes, variable gears, friction clutches in the textile sector, and the production of profiled diamond tools utilized for micro-finishing screw threads, ball-guiding grooves. Ni–P–PTFE–SiC is employed in molds, automotive elements, and general wear components. Ni–W–P–Al_2O_3 offers enhanced thermal stability. Ni–P–B_4C is pertinent to magnetic field applications. Ni–P–Fe_3O_4 caters to high-temperature oxidation requirements.

1.7 Electroless nickel nano-coatings

Electroless nickel nanocoatings are characterized by the thickness of the coating or the presence of second phase particles dispersed within the Ni–P matrix at the nanoscale. The inclusion of fine second phase particles, such as SiO_2, CNT, ZrO_2–Al_2O_3–Al_3Zr, hexaferrites, ferrites, ZnO, Al_2O3–TiO_2, within a metal/alloy matrix has led to the development of a new generation of electroless Ni–P nanocomposite coatings. Over the past decade, numerous researchers have successfully synthesized various electroless Ni–P nanocomposite coatings, with particular focus on combinations like SiC, CeO_2, TiO_2, Al_2O_3, $Zn_3(PO_4)_2$, $ZnSnO_3$, $ZnSiO_3$, single wall carbon nanotubes (SWCNTs), and nanometer diamond (ND). Furthermore, the deposition of electroless Ni–P at the nano level or on nanoscale particles is also referred to as electroless Ni–P nanocoatings.

1.8 Different process of Surface Coating and Surface Modification

Numerous processes exist that entail the application of a material layer, which may not necessarily be metallic, in order to fulfil the demands of particular service conditions. They are,

1.8.1 Physical vapour deposition (PVD)

Physical vapour deposition is a vacuum deposition method used to produce thin films by the condensation of a vaporized form of the desired film material onto various surfaces.At first, the material to be deposited is vaporized using physical means, such as heating (thermal evaporation), sputtering (using ionized gas), or an arc discharge. Then vaporized material travels through a vacuum or low-pressure gas environment from the source to the substrate. After that, the vapor condenses onto the substrate, forming a thin film with precise control over thickness and composition.

1.8.2 Plasma deposition

Plasma Deposition is a process used to deposit thin films onto surfaces by utilizing a plasma to break down gaseous precursors and allow the formation of a solid film on a substrate. It involves the use of a plasma, which is a state of matter characterized by ionized gases, to deposit thin films onto a substrate. First plasma is created by applying energy to a gas or gas mixture in a vacuum chamber. This energy ionizes the gas, creating a highly reactive environment. Then, Gaseous precursors containing the desired film material are introduced into the plasma chamber. These precursors undergo chemical reactions within the plasma, leading to the formation of solid film species. After that, he solid film species condense onto the substrate, forming a thin film. The substrate is typically held at a controlled temperature to optimize film properties.

1.8.3 Chemical vapour deposition (CVD)

Chemical Vapor Deposition (CVD) is a thin film deposition technique used to create high-quality solid materials on a substrate surface by chemical reactions in the vapor phase. Firstly, Gaseous precursors, typically containing the elements needed for the desired thin film material, are introduced into a reaction chamber. Then, the precursors undergo chemical reactions at the substrate surface, leading to the deposition of solid material. After that, the solid material formed by the chemical reactions deposits onto the substrate surface, forming a thin film.

1.8.4 Thermal spraying

Thermal spraying is a versatile coating process used to apply protective or decorative coatings onto surfaces by heating and propelling coating materials in a molten or semi-molten state onto a substrate. At first, the coating material, typically in the form of powder, wire, or rod, is prepared and fed into a thermal spray gun. Then, the coating material is heated to a molten or semi-molten state using various heat sources, such as combustion flames, plasma arcs, or electric

arcs. After that, the molten or semi-molten coating material is propelled towards the substrate using compressed air, inert gases, or a combination of both. Finally, upon reaching the substrate, the coating material impacts and adheres to the surface, forming a cohesive and continuous coating. The rapid cooling of the molten particles results in the solidification of the coating.

1.8.5 Laser cladding

Laser cladding, also known as laser metal deposition (LMD) or laser cladding deposition (LCD), is an advanced manufacturing process used to apply metal coatings or build up metal layers onto substrates. It involves the use of a high-energy laser beam to melt and fuse metal powder or wire onto a substrate surface. At first, the substrate surface is cleaned and prepared to ensure proper adhesion and compatibility with the deposited material. Then metal powder or wire, typically of the same or similar composition to the substrate or desired coating material, is fed into the laser beam's focal point. After that, a high-power laser beam is precisely directed onto the substrate surface, causing localized melting. Simultaneously, the metal powder or wire is fed into the melt pool, where it melts and fuses with the substrate, forming a metallurgically bonded layer. Then, the laser beam is scanned or guided over the substrate surface in a controlled manner, building up successive layers of the deposited material. Each layer solidifies and bonds to the previous layer, gradually forming the desired coating or component. As each layer is deposited, it rapidly cools and solidifies, forming a dense and metallurgically bonded coating or structure. After the deposition process, the coated or built-up component may undergo additional machining, grinding, or surface finishing operations to achieve the desired final dimensions and surface quality.

1.8.6 Anodising

Anodizing is an electrochemical process that converts the surface of a metal, typically aluminium, into a durable, corrosion-resistant, and decorative oxide layer. At first, the aluminium substrate is cleaned to remove any contaminants such as oils, greases, or surface oxides. It may undergo pre-treatment steps such as etching or alkaline cleaning to prepare the surface for anodizing. Then cleaned aluminum substrate is immersed in an electrolyte solution, typically sulfuric acid, which acts as the electrolyte. The substrate serves as the anode (positive electrode) in the electrolytic cell. Then a direct current (DC) electrical current is passed through the electrolyte bath, causing oxidation reactions to occur at the surface of the aluminum substrate. Then oxygen ions from the electrolyte react with the aluminum atoms at the surface, forming a layer of aluminum oxide (Al_2O_3) on the substrate surface. This oxide layer grows inward and outward from the substrate surface, resulting in a

porous structure. After anodizing, the aluminum oxide layer may be sealed to enhance its corrosion resistance and improve its surface properties. Sealing can be done through methods such as hot water sealing, steam sealing, or chemical sealing. Finaly, Anodized aluminum surfaces can be further enhanced with color by dyeing the porous oxide layer. The dye penetrates the pores of the oxide layer, resulting in colored surfaces with excellent durability and fade resistance.

1.8.7 Powder coating

Powder coating is a dry finishing process where a fine powder is applied to a surface electrostatically and then cured under heat to create a durable and decorative finish. At first, the substrate to be coated is cleaned to remove any oil, grease, dirt, or rust. This ensures good adhesion of the powder coating to the substrate. Then powder coating material, which is typically a thermosetting polymer powder, is electrostatically charged and sprayed onto the grounded substrate. The charged powder particles adhere to the grounded surface due to electrostatic attraction. After that, the powder coating application is usually performed in a specialized booth equipped with spray guns, recovery systems, and ventilation to control overspray and minimize powder waste. After the powder is applied, the coated substrate is transferred to a curing oven, where it is heated to a specified temperature. During curing, the powder melts and flows to form a smooth and continuous film. Chemical cross-linking reactions occur within the polymer matrix, resulting in a durable and cured coating. Once cured, the coated substrate is cooled to room temperature. The finished coating is visually inspected for uniformity, adhesion, and any defects.

1.8.8 Galvanizing

Galvanizing is a process used to protect steel and iron from corrosion by applying a zinc coating. At first, the steel or iron substrate undergoes thorough cleaning to remove any oil, grease, or dirt. This is typically done through chemical cleaning or abrasive blasting to ensure proper adhesion of the zinc coating. Then, the substrate may undergo pickling, where it is immersed in an acidic solution (typically hydrochloric acid or sulfuric acid) to remove any existing oxides and mill scale from the surface. After cleaning, the substrate is immersed in a flux solution (usually a mixture of zinc ammonium chloride) to prevent oxidation of the surface prior to galvanizing. The flux also helps in promoting the adhesion of the zinc coating. Then the cleaned and fluxed substrate is immersed into a bath of molten zinc at temperatures typically around 450°C (840°F). The zinc bath may contain small amounts of other metals such as aluminum to improve the coating's properties. When the substrate is immersed in the molten zinc, a metallurgical reaction occurs

between the zinc and the steel substrate, forming a series of zinc-iron alloy layers on the surface. The coating thickness is typically controlled by the immersion time and the withdrawal rate from the zinc bath. After galvanizing, the coated steel is removed from the zinc bath and allowed to cool to room temperature. The coated steel is then visually inspected for uniformity and any defects in the coating.

1.8.9 Electrolytic deposition

Electrolytic deposition coating, commonly known as electroplating, is a process that uses an electric current to deposit a layer of material onto a substrate.

Firstly, the substrate (the object to be plated) is thoroughly cleaned to remove any contaminants. Then, the electrolyte solution contains metal ions of the coating material, such as copper sulphate for copper plating, nickel sulphate for nickel plating, and gold cyanide for gold plating. After that, the substrate is connected to the negative terminal (cathode) of a power supply, while a piece of the coating material (anode) is connected to the positive terminal. Both are immersed in the electrolyte solution. When an electric current is passed through the solution, metal ions from the electrolyte are reduced at the cathode (substrate), depositing a thin layer of the coating material onto the substrate. Simultaneously, metal atoms from the anode dissolve into the electrolyte to replenish the metal ions. After electroplating, the coated substrate is rinsed and may undergo additional treatments such as polishing, annealing, or further protective coatings to enhance the properties of the deposited layer.

1.9 Some Technical Information about Electroless Nickel Deposition Process

1.9.1 General Information

The purpose of various bath components is shown in contrast to most electro-deposition baths, all electroless baths possess certain characteristics which may be summarized as follows:

- The bath is comprised of nickel ions and a reducing agent in a metastable equilibrium. Typically, measures are taken to ensure that the bath is stable enough to prevent spontaneous reactions between the components at standard operating temperatures. Consequently, the stability of the bath holds significant importance.
- The nickel concentration in these solutions is notably low, ranging from 2 to 8 grams per Liter.

- The rate of deposition generally falls within the range of 10 to 25 micrometers per hour, representing a relatively modest speed.
- Apart from the composition of the bath, the rate of deposition is intricately linked to factors such as temperature and pH, and to a certain extent, the age of the bath. Commercial formulations incorporate buffers, complexants, accelerators, and stabilizers to optimize the deposition rate and stability of the bath.
- Metal deposition commences and persists through the action of a catalyst, the removal of which halts the reaction.
- In scenarios where the material to be coated acts as a catalyst itself or has been activated with a catalyst, the surface serves as a catalyst.
- Coatings resulting from electroless deposition typically consist of not only pure metal but also phosphorus or boron, originating from the reducing agent. The quantities of these elements present are contingent upon the deposition conditions. Should heavy metals like titanium, lead, or cadmium be used as stabilizers, they too will become part of the deposit.

1.9.2 Reducing agents for electroless Nickel Deposition

In addition to the nickel salt typically employed, such as the sulphate or the chloride, the primary component of the bath is the reducing agent, leading to the establishment of a classification system based on this factor. The primary reducing agents include hypophosphite, borohydride, amino-boranes, and hydrazine. Among these, sodium hypophosphite ($NaH_2PO_2.H_2O$) emerges as the most prevalent, forming colorless hygroscopic crystals that exhibit high solubility in water. The technical process of its production can be outlined as follows:

$4P + 4OH^- + 4H_2O \rightarrow 4H_2PO_2^- + H_2O$; $4P + 4OH^- + 2H_2O \rightarrow 2H_2PO_3^- + 2PH_3$

The orthophosphate formed as by-product ($H_3PO_3^-$) is precipitated as the insoluble CaH_3PO_3, by addition of $Ca(OH)_2$ The redox potential of the hypophosphite ion is given as-1.065V (at pH = 7) and -0.882V (pH 4.5) while alternative values are -1.57V in alkali and -1.36V in acid medium. On this basis the hypophosphite is one of the strongest reducing agent.

1.9.3 Stabilizing agent

Stabilizers play a crucial role in electroless nickel (EN) plating processes, particularly on magnesium alloys, influencing bath pH, coating quality, and bath life.acetate, as a pH stabilizer, outperforms other stabilizers in buffer

capacity, enhancing EN coating quality and corrosion resistance. Proper usage of ammonium acetate can extend the bath life pH stabilizers like ammonium acetate and ammonium succinate exhibit better buffer performance in the pH range of 4-6, crucial for maintaining optimal plating conditions. Stabilizers help in preventing corrosion spots on coatings, ensuring compact and uniform Ni-P alloy coatings on magnesium substrates. The addition of stabilizers helps in controlling bath pH within the desired range, enhancing the overall quality and longevity of the plating solution.Stabilizers like ammonium acetate are essential for constructing a strong buffer couple in the bath, maintaining the required pH for efficient EN plating processes.

1.9.4 Complexing Agent

In order to prevent the decomposition of the solution and to make the bath stable the complexing agents are added to the electroless bath. It also controls the reaction mechanism, deposition rate so that the deposition occurs only over the catalytic surface. Complexing agents are generally organic acids or their salts; however, there are two exceptions. The first one is the inorganic pyrophosphate anion which is used as a complexing agent exclusively in alkaline EN (Electroless-Nickel) solutions, and the second one is ammonium ion, which is usually added to the plating bath for pH control or maintenance. The complexing agents serve as a buffering agent that prevents the pH of the solution from falling too fast; they prevent the precipitation of nickel salts, e.g., basic salts or phosphites and also reduce the concentration of free nickel ions by forming meta-stable complexes.

1.9.5 Surfactants

Surfactants are compounds that lower the surface tension between two substances, such as a liquid and a solid or between two liquids. They are amphiphilic molecules, containing both hydrophilic (water-attracting) and hydrophobic (water-repelling) regions. In the context of electroless nickel (Ni-P) coating, surfactants like sodium dodecyl sulphate (SDS) play a crucial role in influencing the surface roughness, microhardness, and microstructure of the coated samples. The addition of these surfactants at a concentration of 0.6 g/l results in a smoother surface finish with reduced average roughness values compared to coatings without surfactants. The presence of surfactants during the deposition process enhances the hardness of the coated layers significantly. For instance, with the addition of SDS, the microhardness value increased to 685 Hv, for coatings without surfactants. Surfactants like SDS also impact the microstructure of the deposited layers. They help in dispersing fine nickel particles uniformly on the substrate surface, leading to improved surface finish

and quality of the deposits, ultimately enhancing properties like corrosion resistance.

1.9.6 Effect of Temperature

Temperature is considered the primary factor that significantly influences the rate at which deposition occurs. The majority of acidic hypophosphite solutions typically function within the temperature range of 85°C to 95°C. Conversely, a limited number of hypophosphite solutions with an alkaline to neutral nature have the capability to function across a broad pH spectrum at temperatures ranging from room temperature up to 70°C. It is universally acknowledged that as the temperature rises, the rate of deposition also increases.

1.9.5 Effect of pH

The decrease in bath pH resulted in an increase in the deposition of phosphorus content.

Elevating the pH produces the following consequences:

- Enhanced deposition speed, which is somewhat linearly linked to pH at a specific temperature.
- Alteration of the hypophosphite reaction from catalytic to homogeneous mechanism. Resulting in the potential spontaneous breakdown of the solution leading to nickel deposition.
- Reduction in the solubility of nickel-phosphate. The deposition of undesired components might trigger decomposition, often resulting in uneven deposits.
- Diminishment of the phosphorus content within the deposit.

Decreasing the pH may result in:

- Prevention of basic salts and hydroxides deposition.
- Diminished reductive ability of hypophosphite.
- Improved buffering capacity of species within the bath.
- Below pH 4, there is a delayed deposition rate and potential attack of the deposit by the solution.

1.10 Application of Electroless Nickel Coating

The main application of electroless composite coatings is for machining and finishing tools requiring maximum wear resistance, surface friction coefficient, and hard surface. The applications are shown in table

Table 1.2: Application of electroless Ni–P coatings. [31]

Sl No.	Application avenue	Components
1	Automotive	Heat sinks, carburettor components, fuel injection, ball studs, differential pinion ball shafts, disk brake pistons and pad holders, transmission thrust washers, synchromesh gears, knuckle pins, exhaust manifold sand pipes, mufflers, shock absorbers, lock components, hose couplings, gear and gear assemblies. Fuel pump motors, aluminium wheels, water pump components, steering column wheel components, air conditioning compressor components, decorative plastics and slip yokes
2	Aircraft/ aerospace	Bearing journals, servo valves, compressor blades, hot zone hardware, pistons heads, engine main shafts and propellers, hydraulic actuator splines, seal snap sand spacers, landing gear components, pilot tables, gyro parts, engine mounts, oil nozzle components, turbine front bearing cases, engine mount insulator housing, flanges, sun gears,
3	Chemical & Petroleum	Pressure vessels, reactors, mixer shafts, pumps and impellers, heat exchangers, filters and components, turbine blades and rotor assemble, compressor blades and impellers, spray nozzles, valves, chokes and control valves, oil field tools, oil well valves: ball, gate, plug, check and butterfly, stainless steel packers and equipment, oil well turbine and pumps, drilling mud pumps, hydraulic systems actuators blowout
4	Electrical	Motor shafts, rotor blades of stator rings
5	Electronics	Head sinks, computer drive mechanisms, chassis memory drums and discs, terminals of lead wires, connectors, diode and transistor cans, interlocks, junction fittings and PCB
6	Food	Pneumatic canning machinery, baking pans, moulds, grills and freezers, mixing louts, bun warmers and feed screw and extruders
7	Marine	Marine hardware, pumps and equipment

8	Material Handling	Hydraulic cylinders and shafts, extruders, link drive belts, gears and clutches
9	Medical & Pharmaceuti cal	Disposable surgical instruments and equipment, size ring screens, pill sorters and feed screws and extruders
10	Military	Fuse assemblies, tank tarred bearings, radar wave guides, mirrors, motors, detonators and firearms
11	Mining	Hydraulic systems, jetting pump heads, mine engine components, piping connections, framing hardware
12	Moulds & dies	Zinc dies, cast dies, glass moulds and plastic injection moulds of plastic extrusion dies
13	Printing	Printing rolls and press beds
14	Rail road	Tank cars, diesel engine shafts and car hardware
15	Textiles	Guides, fabric knives, spinnerets, loom ratchets and knitting needles
16	Wood & paper	Knife holder corer plates, abrading plates and machine parts
17	Miscellaneo us	Chain saw engine, Precision tools, Shower blades and heads, Pen tips

Chapter 2:

Literature Review
&
Research Objectives

2.1 Literature Rivew

The research paper focuses on the effects of cobalt content on the mechanical and corrosion properties of electroless Ni-Co-P/Tin nanocomposite coatings on aluminium alloys. Ternary coatings with varying Co content (0-23 wt.%) were successfully deposited on Al alloys, showing enhanced properties with increased Co content. The adhesion force of the coatings increases with higher cobalt content, attributed to good compatibility with the aluminium substrate. Tin particles are successfully co-deposited into the Ni-Co-P matrix, enhancing the properties of the coatings. Cobalt content influences the corrosion resistance of the coatings by affecting passivation behaviour and grain size. Passivation behaviour improves corrosion resistance, with a stable passivity observed in all specimens. The coatings exhibit a compact granular structure with rough surfaces, and the boundary between nodules becomes more pronounced with increased cobalt content. Coatings show good adhesion to the alloy surface without cracks or bubbles at the interface. [1]

Electroless Ni-P coatings are commonly used in various industries due to their exceptional corrosion and wear resistance. Previous studies have shown that the addition of TiO_2 nanoparticles to Ni-P coatings enhances their anti-corrosion and anti-wear properties. However, there is a lack of research on the antibacterial properties of Ni-P-TiO_2 composite coatings, which are crucial for applications in inhibiting biofouling on surfaces like heat exchangers, ship hulls, and pipelines. The incorporation of TiO_2 nanoparticles into the Ni-P matrix is believed to combine the advantages of Ni-P alloy and TiO_2, offering good wear, corrosion resistance, and antibacterial properties. The experimental results of this study demonstrated that Ni-P-TiO_2 coatings significantly reduced the adhesion of bacterial strains, such as Pseudomonas fluorescens, Cobetia, and Vibrio, compared to stainless steel and Ni-P coatings. [2]

The grain size of Ni (111) and Ni3P in the heat-treated Ni-P coating decreased as the TiO_2 particles content increased, ranging from 0 to 5 g/l. The decrease in grain size can be attributed to the distribution of TiO_2 nanoparticles on the boundaries of Ni-grains, which restricts the growth of Ni grains during the

deposition process. After heat treatment, the surface morphology of the coatings changed, becoming more uniform with a needle-like structure due to the presence of TiO_2 nanoparticles. The calculated grain size using the Scherrer method was around 3.0 nm for Ni-P, indicating a small grain size in the coatings. The data showed that the grain size of Ni (111) and Ni3P decreased with increasing TiO_2 particles content, leading to a finer microstructure in the composite coatings. [3]

Nanocomposite coatings have garnered attention due to their distinctive characteristics, such as mechanical, magnetic, and optical properties. Numerous particles have been integrated into metal matrices, including SiC, B_4C, Al_2O_3, ZrO_2, and ceria in micron-scale dimensions. There has been a recent shift in focus towards nanomaterials due to their superior properties. Present investigations in nanocomposite Ni-P plating revolve around the addition of inorganic non-metal nanoparticles like SiO_2, MoS_2, Au, Ag, Al_2O_3, among others. The primary objective of this research is to apply Ni-P-TiO_2 coatings with varying TiO_2 nanoparticle concentrations on low carbon steel utilizing the electroless deposition method. The pH level plays a critical role in the co-deposition procedure, impacting the integration of TiO_2 nanoparticles in the coating. Elevating the pH level improves the reduction process, deposition speed, and particle integration within the coating. The concentration of SDS has a notable influence on the TiO_2 content present in the deposited coatings. An optimal SDS concentration boosts the stability, wettability, and electrostatic attraction of particles, thereby enhancing the quality of the coating.[4]

The scholarly article presents a novel processing paradigm for fabricating nano-structured metal-matrix composite coatings through the amalgamation of sol-gel and electroless plating methodologies. The investigation is centred on the fabrication of Ni-P-TiO_2 nano-composite coatings through the incorporation of transparent TiO_2 sol into the conventional electroless plated Ni-P solution, resulting in enhanced microhardness and wear resistance. Conventional Ni-P-TiO_2 composite coatings, manufactured utilizing solid particle blending techniques, exhibited aggregation of TiO_2 nano-particles, whereas the innovative approach effectively circumvented this challenge, thereby augmenting the particle dispersion strengthening mechanism. The crystalline

state transformation of the composite coatings' phase structure precipitated a notable upsurge in microhardness from 710 HV_{200} to 1025 HV_{200}, consequently enhancing wear resistance. The examination posits that this pioneering processing concept holds vast industrial potentials across diverse metal-oxide composite coating systems. [5]

Numerous research studies have delved into the integration of various particles in electroless Ni-P coatings with the aim of augmenting corrosion protection and physical characteristics. Balaraju and colleagues conducted a comprehensive review on the attributes of electroless Ni-P composite coatings containing diverse particles, shedding light on the factors influencing particle integration and its repercussions on coating properties. The introduction of Al_2O_3 particles into Ni-P coatings was observed to diminish nodularity and slightly lower corrosion current density in a NaCl solution. Investigations on electroless Ni-P-CNT nanocomposites exhibited notable enhancements in wear resistance and reductions in friction coefficients. The inclusion of SiO_2 nanoparticles in Ni-P coatings resulted in enhanced corrosion resistance and micro-hardness. Dehghanian et al. scrutinized the impact of TiC nanoparticles on Ni-P coatings, leading to alterations in morphology and advancements in corrosion resistance. The incorporation of surfactants played a significant role in influencing TiC nanoparticle integration in Ni-P coatings, ultimately bolstering corrosion protection. Research on Ni-P-SiC nanocomposites demonstrated heightened micro-hardness levels and improved corrosion resistance.[6]

The research paper investigates the effects of cobalt content and heat treatment on the mechanical properties of nickel-cobalt-phosphorus (Ni-Co-P) alloys. Various Co contents up to 45 were studied, showing that an increase in Co content leads to improved stabilization of grain size and crystallographic structure upon thermal annealing, enhancing hardness and wear resistance. Electroless deposition was used to fabricate Ni-P and Ni-Co-P alloys, followed by heat treatment, revealing that Co addition enlarges nodular clusters, increases surface roughness, and influences the crystallographic plane orientation, impacting the microstructure and mechanical responses. The study emphasizes

the importance of considering the erosive modes when designing Ni-Co-P alloys for wear-related applications, as different wear mechanisms are observed based on Co content and heat treatment. This literature survey highlights the key findings and methodologies employed in the research paper regarding Ni-Co-P alloys' mechanical properties. [7]

The study focuses on optimizing the hardness of an electroless Ni-Co-P coating using the Taguchi method, with key parameters being the concentrations of Cobalt Sulphate and Sodium Hypophosphite, as well as the temperature of the electroless bath. The response variable in the research is the hardness of the Ni-Co-P coating, which is optimized through a single response optimization process involving the three factors mentioned earlier. The study utilizes the Signal to Noise ratio (S/N) to assess the quality of the coating, with a higher S/N ratio indicating better quality. The Taguchi method employs the S/N ratio in three different ways to evaluate the coating performance. Various analytical techniques such as X-Ray diffraction (XRD), Energy-dispersive X-Ray Spectroscopy (EDAX), and Scanning Electron Microscopy are employed to analyse the composition, phases present, and microstructure of the coating, revealing the presence of Cobalt, Phosphorus, and different phases like Co_2P and Ni_3P. [8]

Electroless Ni-Co-P alloy coatings were applied to reduce the corrosion rate of copper substrates. Central Composite Design (CCD) was utilized to optimize deposition parameters for enhanced corrosion resistance. The corrosion rate was evaluated using the Potential Dynamic test in a 3.5% NaCl solution, and the Tafel plot was employed to determine the corrosion current density for each coated substrate. ANOVA analysis identified significant interactions and key factors affecting the corrosion response of the coatings. The regression analysis demonstrated a good fit of the experimental data with a coefficient of determination (R^2) value of 0.9531 and a significant model F-value of 22.57. The optimized conditions for bath deposition were found to be 15 g/L of Cobalt Sulphate, 30 g/L of Sodium Hypophosphite, and a bath temperature of 80°C to achieve a corrosion rate of 0.535 μm/Y. [9]

Electroless Ni-Co-P ternary alloy deposits were prepared and characterized using various techniques like X-ray diffraction (XRD), differential scanning calorimetry (DSC), thermogravimetric analysis (TGA), and vibration sample magnetometer. The plating rate of these deposits depends on factors like the concentration of sodium hypophosphite, pH of the plating bath, plating time, and the metallic ratio. Increase in the metallic ratio leads to higher cobalt content and lower nickel content in the deposits, while the phosphorus content slightly decreases. The deposits are amorphous initially, with soft magnetic characteristics, and exhibit changes in magnetic properties like saturation magnetization, remanence, and coercivity based on cobalt content. The magnetic properties of the deposits are influenced by the Curie transitions of nickel and non-stoichiometric Ni-Co based alloys, with variations observed with different cobalt contents. [10]

The Ni-Co-P film is widely used in various applications such as magnetic recording media, diffusion barriers, anti-corrosion materials, electromagnetic shielding materials, microwave absorbers, and electrocatalysis materials. Electroless Ni-Co-P films can be deposited on Fe films without the need for sensitization and activation steps. The surface of the deposited film is uniform, and the growth behaviour is influenced by the Co2+ ion concentration in the plating bath. A higher Co2+ ion concentration leads to a decrease in plating rate and an increase in activation energy. The ratio of Co/Ni in the film is generally higher than that in the plating bath, except for specific conditions. Transmission electron microscopy (TEM) is used to characterize the microstructure, thickness, and composition of electroless Ni-Co-P films. The method involves preparing cross-sectional TEM samples and observing the variations in film thickness and microstructure during the growth process. [11]

Electroless Ni-P deposits are widely used due to their excellent properties like high wearability, corrosion resistance, and good electrical and magnetic properties. The addition of cobalt to the Ni-P system can enhance the properties of the deposits. Cobalt improves the coercive force, reduces residual magnetism, and is beneficial for applications requiring high-density disks or electromagnetic shielding films. The study focused on electroless Ni-Co-P

deposits on an Al substrate, analysing their surface morphology, microstructure, composition, corrosion resistance, and electromagnetic shielding properties. It was found that cobalt significantly improved the corrosion resistance and electromagnetic shielding effectiveness of the deposits. The structure of the Ni-Co-P deposits varied with the cobalt content, with deposits 1-3 being amorphous and 4-6 having a mixed crystal and amorphous structure. The deposits exhibited good electromagnetic shielding properties, with all SE values exceeding 60 dB, and the highest SE value was 112.8 dB in high frequency. [12]

Electroless Ni-Co-P coating on pure copper substrate has been studied, focusing on the deposited mass per unit area as the response variable. The influence of process parameters like cobalt source concentration, reducing agent concentration, and temperature on the deposition has been analysed. Statistical analysis and mathematical modelling have been utilized to understand the effects of individual parameters and their interactions on the coating process. The study highlights the transition of the amorphous structure of Ni-Co-P deposits to a crystalline structure post-heat treatment, leading to enhanced hardness and corrosion resistance. Previous research has mainly focused on the impact of individual parameters, emphasizing the importance of statistical analysis and mathematical modelling to comprehend interactions between process variables. The research employed a full factorial design and central composite design to collect data for fitting first and second-order response surfaces, respectively, to predict the deposition rate accurately. [13]

The research paper focuses on the deposition and characterization of amorphous electroless Ni-Co-P alloy thin films for ULSI applications. Electroless deposition of Ni-Co-P alloy thin films was carried out using sodium hypophosphite and sodium citrate in an alkaline plating bath. The study examined the effect of solution pH and temperature on the plating rate, showing a decrease in activation energy with an increase in pH of the plating bath. Post-deposition annealing at temperatures approaching 400 °C led to a significant decrease in sheet resistance of the alloy thin films. XRD analysis revealed the presence of nickel and nickel phosphide peaks, with a transition from metastable phases to thermodynamically stable phases after annealing at 600

°C, indicating crystallization of the thin films. Surface topography analysis showed variations in grain size ranging from 20-40 nm. [14]

Electroless deposited Ni-P and Ni-Co-P thin films were studied for their diffusion barrier properties in ULSI technology. Both Ni-P and Ni-Co-P films exhibited thermal stability up to 500 °C against Cu diffusion, with the formation of various silicide phases upon further annealing. Ni-Co-P films with increased Co content are suggested to enhance the diffusion barrier properties by blocking grain boundary diffusion paths for copper. The presence of Cobalt in Ni-Co-P films was confirmed by EDX data, although XRD did not show Co peaks. Ni-P films showed barrier failure at 500 °C, evidenced by the appearance of Cu_3Si peaks and increased sheet resistance. [15]

Ni-Co coatings are well-known for their exceptional properties like high strength, good wear resistance, corrosion resistance, and unique magnetic properties. Electroplating is preferred over electroless plating due to its ease of operation and accurate deposition rate control. Ni-Co coatings have been extensively used in electronic devices like computer hard drives for several decades. The addition of TiO2 nanoparticles in Ni-Co coatings enhances wear resistance by improving hardness and acting as a solid lubricant during wear. The microstructure, mechanical properties, and corrosion resistance of Ni-Co-TiO2 composite coatings are influenced by the concentration of TiO2 nanoparticles, with an optimum at 10 g/L. XRD analysis of the coatings revealed a face-centred cubic lattice structure with preferential (111) growth orientation and the presence of TiO2 nanoparticles in the composite coatings. [18]

Artificial Neural Networks (ANN) have been effectively utilized in various fields, including the evaluation of electroless coatings properties. Limited studies have focused on optimizing and predicting electroless coating bath parameters to achieve maximum deposition rates in Ni-W-P-nanoTiO2 composite coatings. The research paper explores the experimental study of Ni-W-P-nanoTiO2 composite coatings on API X60 low-carbon steel using the electroless method. Taguchi design (L9 orthogonal array) was employed to optimize electroless bath parameters for maximum deposition rate, with confirmation tests validating the optimal parameters. Surface morphology was characterized using Atomic Force Microscopy and Field Emission Scanning Electron Microscopy, while compositional and phase analysis was conducted

using Energy-Dispersive Spectroscopy and X-ray Diffraction. Corrosion behaviour of the nanocomposite coatings was evaluated in 3.5 wt.% NaCl solution through potentiodynamic polarization, showcasing improved corrosion resistance due to the semi-crystalline nature of the coatings and the presence of tungsten and TiO2 nanoparticles.[22]

2.2 Scope of Present Work

The literature review done above clearly reflects that the characteristics of Ni-Co-P and Ni-P-TiO_2 coating have currently become an active field of research. Especially due to its superior qualities as a coating material than Ni-P, the former has created a huge impact among the enthusiasts in this field. Many scientists and researchers have already had much contribution in this regard as seen in the literature review. Although there have already been many contributions in the study of Ni-Co-P and Ni-P-TiO_2 as a coat material. some areas still need to be enlightened more clearly. One of the areas that still offers substantial opportunities for research relates to the tribological characteristics observed when combining two different coating materials. It is seen through the literature review that a very little work has been done in this regard and almost no work has been done to Ni-Co-P-Tio_2 coatings and its synthesis. The present work is a humble attempt in that direction.

2.3 Objective of the present work

The current investigation will focus on examining the hardness of electroless Ni-Co-P-TiO_2 quaternary alloy coating on a Mild Steel substrate. Thus, the aim of this study will be directed towards the subsequent objectives:

- Synthesis of Electroless Ni-Co-P-TiO_2 quaternary alloy coating on Mild Steel substrate.
- Measurement of hardness and electroless Ni-Co-P-TiO_2 coating.
- Optimizations of one variable, specifically the hardness of the coating, through the variation of coating process parameters.
- Application of the Taguchi method for parametric optimization.
- Exploration of the microstructure and composition of Ni-Co-P-TiO_2 coating using Scanning Electron Microscopy (SEM) and Energy dispersive X-ray analysis (EDAX) respectively.

Chapter 3:

Experimental Details

The current investigation explores the preparation and characterization of Ni-Co-P-TiO2 electroless quaternary alloy coatings. These particular coatings are applied onto substrates made of Mild steel. The process of coating deposition, in addition to various parameters and the resulting hardness properties, have been examined for these coatings, followed by the optimization of said coatings. The surface morphology, phase transformation characteristics, and chemical composition of the coatings have been analysed using scanning electron microscopy (SEM), X-ray diffraction (XRD) analysis, and energy dispersive X-ray spectroscopy (EDX), respectively.

3.1 Deposition of Electroless Ni-Co-P-TiO_2 Coating

3.1.1 Preparation of substrate sample

Wire EDM is initially employed in the process of cutting the Mild steel plate into smaller dimensions measuring (10×6×2) mm^3, which serve as substrates utilized for the application of Ni-Co-P-TiO_2 coatings. Subsequently, the substrate is subjected to polishing using various SiC papers with grit sizes of 220, 400, 600, 800, 1000, 1200, and 1500 respectively in order to attain a refined surface finish prior to commencing the coating deposition procedure. Following this, the substrate undergoes ultrasonic cleaning in acetone for a duration of 8-10 minutes, and subsequently, it is rinsed with distilled water for 2-3 minutes. An essential aspect in the preparation of samples is the activation step, where samples are treated with a solution of Palladium chloride ($PdCl_2$) for a period of 8-10 seconds at a temperature of 55°C, and then washed with distilled water for a brief duration. Subsequent to surface activation, the samples are submerged in an electroless bath.

3.1.2: Experimental set up for Ni-Co-P-TiO2 Electroless Coating

The following instruments and chemical were required for obtaining electroless coating deposition:

(i) Electronic Balance: High precision electronic balance was used to measure weights of substrates and chemicals. AFCOSET, Model No. ER-182A, SL. No. 0108017, Maximum range 180 g, Minimum range 0.01 mg shown in Figure 3.1

(ii) Magnetic Stirrer cum heater: Magnetic stirrer cum heater was used for proper mixing of the bath solution and to heat the bath to the required

temperature. 2MLH Magnetic stirrer, manufactured by Remi Instruments shown in fig 3.2 was used.

(iii) Mercury in glass Thermometer: Thermometer is used to maintain the bath temperature during the coating process.

(iv) Glass Beakers: It is used to hold the bath solution (BOROSIL).

(v) pH meter: A digital pH meter was used to measure the pH of the electroless bath. Electronics India, Model No. 181, SL. No. 11505265, Maximum range 14 pH, Minimum range 0.01 pH shown in Figure 3.3.

(vi) Ultrasonic cleaner: Ultrasonic cleaners are used to clean many different types of objects, including industrial parts, tools, coins, the ultrasonic cleaner effectively removes contaminants from various objects, ensuring a thorough cleaning process in industrial applications shown in Figure 3.4.

Fig-3.1: Electronic Balance

Fig-3.2: Magnetic Stirrer with hot Plate

Fig 3.3: pH Meter

Fig 3.4: Ultrasonic cleaner

3.1.3 Bath preparation and deposition of obtaining Ni-Co-P-TiO_2 Electroless coating

- Nickel Sulphate hexahydrate ($NiSO_4.6H_2O$) served as the primary reservoir of nickel ions in this study. The utilization of nickel sulphate solution played a critical role in furnishing the necessary nickel ions for the electroless coating deposition procedure.
- Cobalt Sulphate ($CoSO_4.6H_2O$) served as a precursor of cobalt ions within the context. The solution of cobalt sulphate contributed significantly to the provision of cobalt ions necessary for the electroless deposition process in conjunction with the nickel sulphate solution.
- Sodium Hypophosphite ($NaH_2PO_2.H_2O$) served as a reducing agent in the conducted experiment. Its role encompassed providing phosphorus as the reducing agent, thereby initiating the reduction process. The electroless plating methodology hinges on a reduction reaction, whereby the oxidization of the reducing agent occurs, leading to the reduction of Ni^{2+} ions which subsequently precipitate onto the surface of the component.
- Tri-sodium Citrate Dihydrate ($Na_3C_6H_5O_7.2H_2O$) was employed as a complexing agent to regulate the kinetics of free metal ion liberation during the process of reduction.
- Ammonium Sulphate $(NH_4)_2So_4$ was used a complexant to maintain bath pH
- Titanium dioxide (TiO_2) was employed as nanoparticle of average particle size of 25nm for composite coating.
- Sodium dodecyl sulphate (SDS) was employed as a surfactant in order to facilitate the suspension and stable dispersion of nanoparticles, prevent the agglomeration of nanoparticles, and regulate the size of the nanoparticles owing to their electrostatic repulsion characteristics.

3.1.4 Steps of Coating

- The initial step involves quantifying the chemical substances as delineated in table 3.1, followed by the combination of Nickel sulphate and copper sulphate with 80 ml of distilled water (DI). Subsequently, there is a need to precisely agitate the solution until the Nickel sulphate is entirely dissolved in the distilled water.

- Thereafter, blend Sodium Hypophosphite, Tri-sodium Citrate Dihydrate, Ammonium Sulphate with 80 ml of DI utilizing a stirrer until complete dissolution is achieved, ensuring uniformity in the solution for the electroless plating procedure. The subsequent stage entails heating the solution to 80°C while adjusting the pH of the bath to 5.6 (±0.2).
- In a another beker TiO_2 and SDS is mixed with 80 ml of DI and put the beker in Ultrasonic Cleaner for 1 hour to proper mixing of TiO_2 and SDS.
- Following this, the sample is activated in a palladium chloride ($PdCl_2$) solution for 8-10 seconds at a temperature of 55°C and then rinsed with distilled water briefly. Post this step, the samples are submerged in the previously made Ni-Co-P solution, allowing the coating process to occur for 30 minutes.
- After the 30-minute coating of Ni-Co-P, the prepared TiO_2 solution is gradually mixed and the magnetic stirrer is introduced at a speed of 300-350 rpm, with a waiting period of approximately 30 minutes.
- Subsequent to the completion of the coating process, the samples are purified with distilled water (DI) and air-dried.
- The representation of the coating process can be observed , while table 3.1 illustrates the quantities utilized in this experimental investigation.

Bath composition	**Quantity**	**Operating conditions**	
Nickel (II) Sulfate ($NiSO_4.6H_2O$)	15-35 (g/L	pH	5.6 (±0.2)
Cobalt Sulfate ($CoSo_4.6H_2O$)	6-14 (g/L)		
Sodium Hypophosphite Hydrated ($NaH_2PO_2.H_2O$)	20-30 (g/L)	Time (minutes)	60
Tri-Sodium Citrate ($Na_3C_6H_5O_7.2H_2O$)	60 (g/L	Speed (rpm)	500
Ammonium sulfate ($(NH_4)_2SO_4$)	40 (g/L)	Bath Volume (mL)	200
TiO_2 nanoparticles	1-3 (g/L)	Temp (°C)	80
Sodium dodecyl sulfate ($C_{12}H_{25}OSO_2ONa$)	0.1 (g/L)		

Table 3.1: Ni-Co-P-TiO_2 composite coating bath composition and coating conditions

3.2 Heat treatment

Heat treatment assumes a pivotal role in modifying the characteristics of Ni-Co-P-TiO_2 composite coatings. The heat treatment process of the Ni-Co-P-TiO_2 amorphous coating entails annealing at varying temperatures (200, 400, 600 degrees Celsius) to stimulate microstructure evolution and phase transition. The mechanical properties of the coating, such as hardness, elastic modulus, and wear resistance, undergo significant influence from the microstructure evolution and phase transition during crystallization induced by heat treatment. Optimal heat treatment procedures lead to enhancements in the hardness, elastic modulus, and wear resistance of the coating. The rate of crystallization product formation in the Ni-Co-P-TiO_2 coating relies on the temperature and duration of heat treatment, with elevated temperatures expediting atom diffusion and fostering nucleation and growth rates of precipitates. The process of heat treatment stands as a fundamental aspect for comprehending the behaviour of composite coatings under diverse thermal circumstances. Utilization of Scanning Electron Microscopy (SEM) aids in observing the alterations in surface morphology subsequent to heat treatment, thereby unveiling changes in grain structure. Energy Dispersive X-ray Analysis (EDAX) facilitates the verification of the presence of various elements like nickel, cobalt, phosphorus, titanium, and oxygen in the coatings following heat treatment. The friction coefficient of composite coatings is impacted by heat treatment, with a rise in friction coefficient observed with the inclusion of TiO_2 particles and higher annealing temperatures, consequently affecting the tribological performance.

3.3 Measurement of Hardness

3.3.1 Hardness properties

Hardness serves as a crucial mechanical attribute frequently utilized for evaluating the quality of coatings. The Vickers hardness number (VHN) represents a common metric of hardness, which is specifically defined as the ratio of the load applied to the total area of the resulting indentation. The absolute hardness (H0) denotes the macro-hardness that remains unaffected by the applied load, exhibiting variations based on a distinct relationship with the load magnitude. The utilization of hardness testing is widespread due to its straightforwardness in approximating the mechanical characteristics of coatings. Particularly within the microhardness characterization range, the hardness number demonstrates variability in response to the applied load, consequently affecting the recorded values. Calculations of composite hardness entail the consideration of factors such as film thickness, indentation imprint, substrate hardness, and their alterations in response to the applied load. The application of

the area law of mixture in microhardness is deemed suitable for thick hard coatings or indentation depths comparable to the film thickness when employing adjusted models. The ratio of indentation depth to film thickness holds significance in elucidating the behaviour solely attributable to the coating properties. Hardness attributes assume a significant role in the characterization of materials, notably in coatings and thin films, thereby influencing diverse industrial applications and material design procedures. The composite hardness level is subject to the influence of both the relative indentation depth and the hardness values of the substrate and coating. An outlined mathematical model suggests that the composite hardness can be expressed as a function of the relative indentation depth, as well as the hardness characteristics of the substrate and coating, with a parameter X incorporated to describe various properties like coating brittleness and indenter geometry. The representation of hardness in terms of the total indentation energy is also feasible.

3.3.2 Hardness measuring machine

Hardness of electroless nickel is a very important factor in many successful applications. In the Vickers microhardness machine Ni-Co-P-TiO2 coated mounted sample is taken as per ASTM standard E384-16 using a hardness tester fitted with a diamond indenter that is four apex angles between opposite sides of 136° (+-5'). A load of 10 gf is applied while the dwell time and indentation speed are kept at 10 s and 25µm/s respectively. An average of 5 hardness values is acquired from the microhardness tester. The indentation depth should be 10-20% of the coating thickness in order to avoid the substrate's effect on hardness. The Vickers's hardness was calculated by using the following equation:

$$HV = \frac{1.8544F}{d^2}$$

Where, F is load in gram and d is the mean of two diagonals created by pyramidal indent in millimetre.

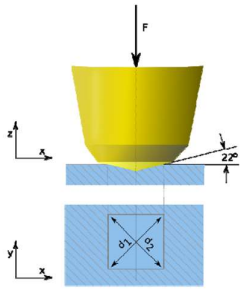

Fig.3.5: Schematic diagram of Vickers Hardness Indentation

3.4 SEM for study of Microstructure and composition

The Scanning Electron Microscope (SEM) Fig 3.6 provides enlarged images depicting the dimensions, morphology, composition, crystallography, and various physical and chemical attributes of a specimen. In the field of material sciences and surface sciences, SEM is employed to magnify surface structures for comparative analysis. By utilizing an electron beam within a vacuum environment and refining it through electromagnetic lenses, SEM enables the generation of high-resolution images. Image formation in the microscope occurs through the detection of reflections or electrons resulting from the interaction between the electron beam and the specimen. A comprehensive evaluation of a coating necessitates the determination of parameters such as grain size, grain orientation, presence of inclusions, and voids at the coating-substrate interface. Key aspects in a typical microstructural examination of a coating encompass the grain arrangement, crystalline phase of the coating and substrate, the coating-substrate interface, and the external coating surface. Optimal microstructural assessment often involves the concurrent application of diverse microscopy techniques, such as Optical Microscopy and Scanning Electron Microscopy.

Energy Dispersive X-ray Analysis (EDAX) primarily serves to conduct elemental analysis of materials by detecting characteristic X-rays emitted upon bombardment with high-energy electrons. This analytical tool facilitates the identification of the elemental composition and the weight percentage of elements within the sample.

EDAX yields quantitative insights into the elemental constitution of the material under scrutiny, aiding researchers in discerning its properties and attributes. The current investigation focuses on the compositional analysis of an electroless nickel coating, with a specific emphasis on determining the presence of nickel and the principal alloying element (phosphorous, nickel, or copper) based on their respective weight percentages. This analysis serves to enhance the understanding of the coating's distinctive characteristics.

Fig- 3.6: Scanning Electron Microscope (SEM)

3.5 Phase Structure Analysis using XRD

X-ray diffraction methodologies are robust and non-invasive instruments utilized for the characterization of materials with minimal sample preparation. XRD offers essential insights into various material properties, encompassing phases, crystalline configuration, average crystallite dimensions, micro and macro strain, orientation parameter, texture coefficient, degree of crystallinity, and crystal imperfections. The principle behind X-ray diffraction lies in the capacity of X-rays to undergo diffraction by a crystalline framework due to their wavelength being akin to the inter-planar spacing within a crystal lattice. The resultant diffraction pattern is distinctive to a particular crystalline arrangement, rendering XRD particularly advantageous for analyses in the realm of inorganic chemistry. The utility of X-ray diffraction spans across a broad spectrum of material characterization applications, ranging from determining crystal structures and orientations to identifying phases and pinpointing trace elements within a substance. Notably, the technique enables the clear differentiation of metal oxides, nitrides, carbides, and sulphides. A standard diffractometer comprises an X-ray generator, a specimen holder with rotational capability, and an array of detectors for monitoring diffracted intensities. The X-rays employed are monochromatic, distinguishing them from those utilized in imaging purposes. By rotating the sample, the diffracted pattern can be discerned, manifesting as alternating dark and light bands indicative of the constructive and destructive interference between scattered X-rays. The angular separation between these bands serves as a gauge for the inter-planar spacing, thereby facilitating compound identification.

3.6 Design of experiments (DOE)

In the domain of statistics and research, the concept of Design of Experiments (DOE) is characterized as a systematic methodology for planning, executing, evaluating, and interpreting the potential results of an experiment by taking into account the input process parameters at varying levels. This approach proves to be effective in examining the correlation between factors (input variables) and responses (output variables), thereby facilitating the optimization of process parameters leading to data-informed decision-making. Consequently, this knowledge serves as a foundation for constructing statistical models aimed at forecasting process performance, by defining the specific levels of settings for combinations of elements where the various experiment runs are to be conducted.

In scenarios where the quantity of combinations in a full factorial design becomes overly extensive, the adoption of a fractional factorial design might be contemplated, wherein certain combinations are excluded. For instance, in a situation where there are 8 factors at two levels, a total of 256 combinations would be generated. The execution of such a vast number of experiments proves impractical due to financial or resource limitations. Therefore, fractional factorial designs come into play, selecting a subset of factor combinations for testing purposes, yielding insights into main effects and certain interaction effects while reducing the number of experimental trials. However, this design loses appeal when a researcher aims to incorporate more than two levels. Efforts are directed towards utilizing the full factorial design of experiments and the analysis of variance methodology to explore the impact of process parameters on output response variables.

Design of Experiments (DOE) is often highly effective in situations where there is a need to: ·

- Enhance the optimization of both product and process designs.
- Investigate the impacts of various factors on overall performance outcomes.
- Resolve issues in production through the systematic layout of experiments.
- Examine the influence of individual factors on system performance.
- Evaluate the importance of each factor on the response of the system.
- Determine the tolerance levels of these factors.
- Allocate resources for quality assurance based on empirical data.
- Determine whether a supplier's component is causing issues.
- Determine the optimal combination of different factors to achieve the most favourable outcomes.

3.6.1 Importance of Design of Experiment (DOE)

Sciencetist Ronald A. Fisher elucidated some fundamental principles of experimental design, among which are

- Randomization: This method serves to counteract potential biases that could influence experimental outcomes, ensuring comparability among groups. It plays a crucial role in managing extraneous variables and facilitating valid statistical inferences.
- Replication: By conducting multiple independent experimental trials or observations under identical conditions for each treatment combination, replication aids in estimating experimental errors, evaluating variability, and enhancing result accuracy and reliability. Replication becomes particularly valuable in scenarios where noise stems from uncontrollable nuisance variables, leading to an improved signal-to-noise ratio.
- Blocking: Employed to diminish variation in experimental units resulting from irrelevant sources, blocking entails the grouping of similar experimental units and the random assignment of treatments within each group.
- Orthogonality: Designs that exhibit orthogonality are characterized by independent or uncorrelated effects of different factors. This property enables efficient estimation of main effects and factor interactions, facilitating the acquisition of clear and unambiguous insights into the impact of individual factors on the response variable.

3.6.2: Application of DOE

Design of Experiments (DOE) is utilized in a wide range of fields, such as manufacturing, engineering, healthcare, agriculture, and social sciences. Some typical applications of DOE are as follows:

- Optimization of processes: DOE facilitates the identification of crucial process factors influencing the process outcome and the determination of optimal levels for these factors, thereby optimizing manufacturing processes. Through systematic manipulation of variables and measurement of responses, researchers can unveil the best settings that lead to enhanced product quality, efficiency, or cost-effectiveness.
- Optimization of costs: DOE contributes to cost optimization by recognizing the principal factors influencing cost variations and ascertaining their optimal levels. This aids in achieving cost savings without compromising quality or performance.
- Improvement of quality: DOE can be utilized to pinpoint critical process parameters and their optimal settings that exert the most significant

influence on product quality. By minimizing variability and comprehending the effects of different factors, organizations can elevate product reliability and consistency, reduce defects, and ensure customer satisfaction.

- Analysis of root causes: When diagnosing a process or system, DOE can be systematically employed to investigate potential causes of an issue. Through manipulation of suspected factors contributing to the problem, researchers can pinpoint the root cause and devise suitable remedies.
- Sensitivity analysis: DOE enables the assessment of a process or system's sensitivity to various factors. By methodically altering the factors, researchers can evaluate which ones wield the most substantial impact and allocate resources to those of utmost importance.
- Development of products: DOE is applied to enhance product formulations or designs by analysing the impact of various factors, including materials, design parameters, or production methods, on the final product's quality or performance. This contributes to the creation of superior products with reduced development time
- Testing for robustness: DOE assists in evaluating the robustness of a process or product design by deliberately introducing variations in operating conditions or component specifications. This aids in determining the conditions under which the process or product reliably performs.
- Scientific investigation: In scientific inquiries, DOE aids researchers in exploring hypotheses, investigating relationships between variables, and establishing cause-and-effect associations. It facilitates controlled experimentation, minimizes bias and confounding variables, and enables the formulation of more dependable conclusions.

3.7 Taguchi Method

The Taguchi method is crucial for achieving robustness in product and process designs, benefiting various stakeholders such as manufacturers, suppliers, and consumers. Taguchi's approach involves defining a loss function influenced by the type of quality characteristic, such as smaller-is-better, larger-is-better, or target-is-best, and determining a performance measure like signal-to-noise (S/N) ratios for optimal controllable factor settings. Taguchi recommends a three-stage design process: system design, where product characteristics are selected based on objectives; parameter design, where optimal control parameter settings are determined to reduce variability; and the formulation of an appropriate SN ratio. The Taguchi method focuses on robust design, minimizing variation with respect to noise factors, and employs

orthogonal arrays in experimental designs for data analysis with a modest number of runs. Criticisms of the Taguchi method include concerns about the performance measure formulation and the need for further research to address issues like the simultaneous effect of factors on mean response and variability. [20]

3.7.1 Analysis of Variance (ANOVA)

The examination of variance through statistical analysis (ANOVA) has been conducted to forecast the statistical significance of the process parameters. It aids in ascertaining the impact of each individual parameter on the output parameter. ANOVA facilitates the formal examination of the significance of all primary factors and their interactions by juxtaposing the mean square with an approximation of the experimental errors at specific confidence levels. Within this study, the optimum hardness, which is influenced by quantity of parameter, is assessed through the ANOVA standard procedure employing the mean values. The proportion of contribution from each process parameter is determined utilizing the ANOVA approach. [21]

3.7.2 Signal-to-Noise ratio (S/N Ratio)

The SN ratio can be basically understood as the ratio of signal factor to the noise factor in the experiment. As per the goal of the optimization, SN ratio can be decided to be maximized, minimized or kept at nominal value. It helps in choosing the control levels that can compensate the effects of noise to the maximum [23]. Here, SN ratio is chosen to be kept the maximum, as the goal of the design.

3.7.3 Experiment Parameters and Response for Taguchi Method

For conducting the experimental analysis, three levels and four control factors were selected, as presented in Table 3. Taguchi L9 (3ˆ4) orthogonal design given in Table 4 was selected to understand the effect of individual factors on Hardness. The four input factors are Nickel Sulphate(A), Cobalt (B), Sodium-hypophosphate (C), TiO_2 nanoparticles (D). Three different levels low (-1), medium (0), and high (+1) were considered based on some preliminary experiments. MinitabR2019 was used for the analysis of Taguchi's design. The response, Hardness of the composite coating was considered for maximum hardness thus S/N ratio (dB) with the "***larger-the-better***" characteristic was calculated using Equation. Finally, a confirmation test (at optimum parameter combination) was performed for validation of the Taguchi optimal parameters.

$$S/N \text{ ratio, “larger - the - better“} = -10 \times \log_{10}\left(\frac{1}{n}\sum_{i=1}^{n}\frac{1}{y_i^2}\right)$$

where n is the total number of experiments and y_i is the observed response for the *i*th number of experimental data for each experiment.

Control Factors	Designation	Unit	Parameter Level		
			-1	0	1
Nickel Sulphate	A	g/L	3	5*	7
Sodium-hypophosphate	B	g/L	4	5*	6
Cobalt Sulphate	C	g/L	1.2	2*	2.8
TiO_2 Nanoparticle	D	g/L	0.2	0.4*	0.6

Table 3.2: Control factors and levels of the parameters

**Mid-level combination as the initial parameter*

Run No	A	B	C	D
1	3	4	1.2	0.2
2	3	5	2	0.4
3	3	6	2.8	0.6
4	5	4	2	0.6
5	5	5	2.8	0.2
6	5	6	1.2	0.4
7	7	4	2.8	0.4
8	7	5	1.2	0.6
9	7	6	2	0.2

Table 3.3: Un-coded experimental plan using Taguchi L9 Orthogonal Array design

Chapter 4:

Results and Discussion

4.1 Introduction

This chapter outlines the findings and discussions regarding the optimization of coating process parameters for electroless Ni-Co-P-TiO_2 coating. The examination was conducted to enhance the coating process parameters for achieving optimal micro hardness. The analyses were performed to identify the appropriate combination of coating process parameters for each response. Subsequently, the Taguchi method was utilized to optimize single performance characteristics for micro hardness, and the corresponding suitable process parameters combinations were documented.

Upon establishing the appropriate process parameters combination, confirmation tests were carried out for all the optimal combinations as compared to the initial process parameters combination to verify their effectiveness. Subsequently, the outcomes of Energy Dispersive X-ray Analysis (EDX) and Scanning Electron Microscopy (SEM) analysis are deliberated. The EDX analysis was conducted to determine the precise composition of elements present in the coating.

4.2 Effect of Micro-Hardness

The current research delves into the examination of the hardness exhibited by the Ni-Co-P-TiO_2 coating applied onto Mild steel through electroless deposition. The results illustrating the hardness values obtained from each experimental trial are presented in the study shown in Table 4.1.

Run No	A	B	C	D	Hardness ($HV_{0.025}$)
1	3	4	1.2	0.2	378
2	3	5	2	0.4	334
3	3	6	2.8	0.6	353
4	5	4	2	0.6	406
5	5	5	2.8	0.2	439
6	5	6	1.2	0.4	511
7	7	4	2.8	0.4	418
8	7	5	1.2	0.6	373
9	7	6	2	0.2	483

Table 4.1: Hardness for Each Run

4.3 Experimental Analysis

4.3.1 S/N Ratio Analysis

Table 4.2 illustrates the hardness and Signal-to-Noise ratio for each individual trial conducted according to the Taguchi L9 orthogonal Array Design.

Run No	Hardness ($HV_{0.025}$)	S/N Ratio
1	378	51.55
2	334	50.48
3	353	50.96
4	406	52.2
5	439	52.85
6	511	54.17
7	418	52.42
8	373	51.43
9	483	53.68

Table 4.2: Hardness and S/N ratio for each run

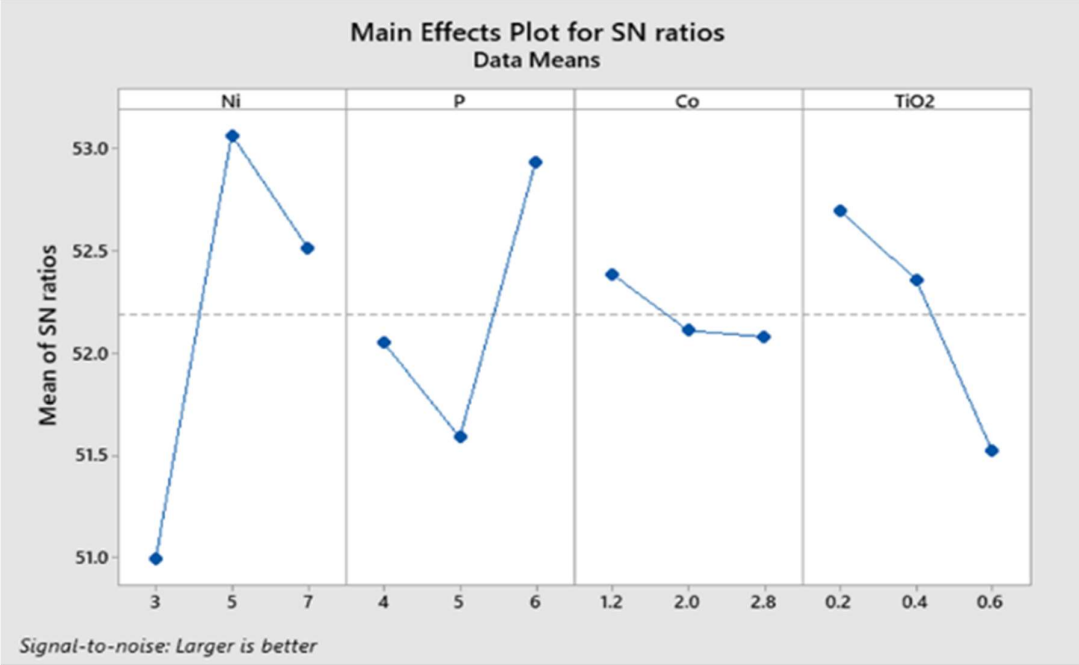

Fig 4.1: Main effect plot for S/N ratios

The main effects of hardness plot (Fig. 4.1) can be interpreted to find which factors play a more significant term in determining the hardness of the coating.

Notation	Parameters	Mean S/N ratio			Max-Min	Rank
		Level 1	Level 2	Level 3		
A	Nickel Sulphate	50.99	53.06	52.51	2.07	1
B	Sodium-hypophosphate	52.05	51.59	52.93	1.35	2
C	Cobalt Sulphate	52.38	52.11	52.08	0.31	4
D	TiO_2 Nanoparticle	52.69	52.36	51.52	1.17	3

Table 4.3: Mean signal-to-noise ratio for Hardness

Table 4.3 depicts the rank of each parameter, which shows that the Nickel Sulphate has the most significant effect, the second most influential parameter is the reducing agent followed by the Nanoparticles while the Cobalt content has the least significance. Therefore, the Taguchi A2-B3-C1-D1 (optimum predicted parameter) combination achieved the maximum Hardness, i.e., mid-level of A (Nickel Sulphate =25 g/L), the highest level of B (Sodium-hypophosphate = 25 g/L), lower level of C (Cobalt= 6 g/L), lower level of D (TiO_2 = 1 g/L).

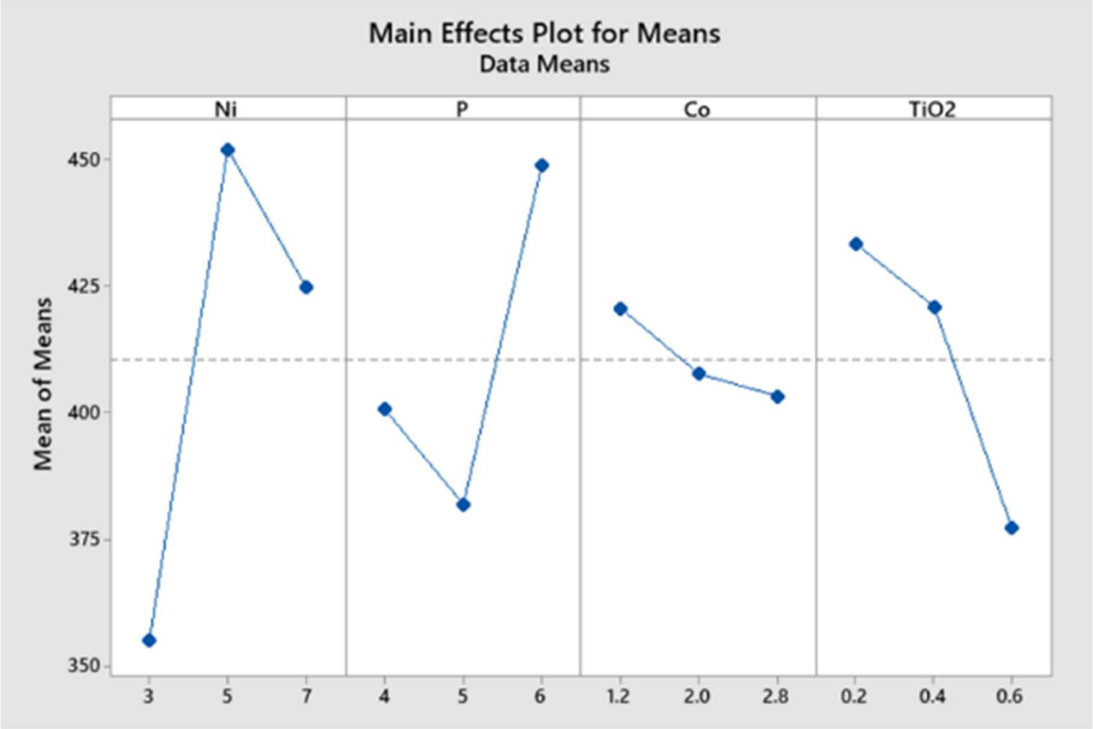

Fig 4.2: Main effect plot for means.

Figure 4.2 shows the main effect plot for means, which depicts the influence of control factors on the deposition rate of Ni-Co-P-TiO_2 coatings. The increase in reducing agent content (B), increases the Hardness. The higher hardness is due to the oxidation of hypophosphite anions. The effect of TiO_2 nanoparticles (D) shows that maximum Hardness was obtained at a lower level of TiO_2 content and the hardness decreases while TiO2 content is increasing. The factor (A) from the Fig 3.1 shows Hardness increases with the increasing content (A) but further increment beyond the mid-level it begins to decline. The effect of Cobalt Content (C) shows that maximum hardness was obtained at lower level and starts decreasing while Cobalt Content (C) is increasing.

4.3.2 Analysis of ANOVA

Parameter	DOF	Sum of Squares	Mean Square	F ratio	% Contribution
A	2	6.8919	6.89192	-	57.11
B	2	2.8164	2.81637	-	23.34
C	2	0.1721	0.17210	-	1.43
D	2	2.1868	1.09341	-	18.12
Error	0	-	-	-	
Total	8	12.0672			100

Table 4.4: Analysis of variance (ANOVA) for Hardness

Parameter	DOF	Sum of Squares	Mean Square	F ratio	P-value	% Contribution
A	2	6.8919	6.89192	40.04590354	0.02*	57.11
B	2	2.8164	2.81637	16.36490413	0.05	23.34
{C}	{2}	{0.1721}	-	-	-	-
D	2	2.1868	1.09341	12.70656595	0.072	18.12
Pooled Error	2	0.1721	0.17210	-	-	1.43
Total	8	12.0672	-	-	-	100

Table 4.5: Pooled ANOVA for deposition rate **(the pooled factor is shown in{})**

*Confidence level = 95%, *Significant (P-value < 0.05)*

The ANOVA provides performance characteristics of the process parameters [24]. ANOVA for the SN ratio based on hardness is shown in Table 4.4. It suggests that the hardness is highly influenced by the Nickel content with a 57.11% contribution followed by reducing agent, TiO_2 nanoparticles content and Cobalt content respectively. The least influential factor indicated by the ANOVA result in Table 4.4 is C (Cobalt content) which contributed 1.43%. Each parameter has 2 degrees of freedom (DOF), making a total DOF of 8. Therefore, the DOF of the error term and mean square or variance of the error term could not be evaluated. Hence, the F-ratio could not be calculated, as the F-ratio is defined as the mean square or variance of individual factors divided

by the variance of the error term [25-27]. To exclude the zero DOF from the error term, a pooled ANOVA is applied. The process of ignoring the least contributing factor is called pooling [27]. Pooled ANOVA shown in Table 4.5 indicates that factor A was highly significant (P-value < 0.05). The P-value is the probability of the parameters having a significant effect on the responses. According to the ANOVA, a factor will be considered statistically significant if its P-value is less than 0.05 at a 95%confidence level [28,29].

The optimal hardness obtained from this experiment is (A2-B3-C1-D1). The hardness for these optimal parameters was found to be 425HV$_{0.025}$

4.3.3 Study of Scanning Electron Microscopy (SEM)

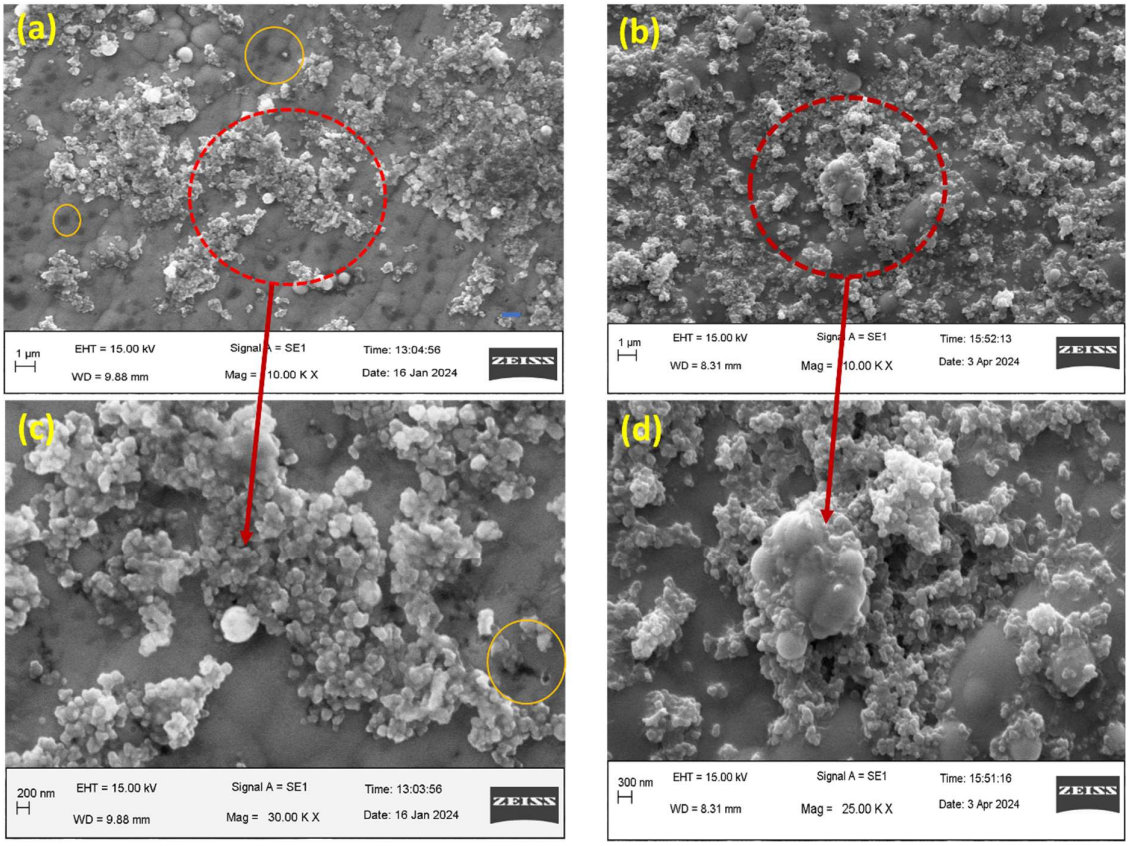

Figure 4.3: SEM morphology of Ni-Co-P-TiO_2 composite coatings a, c initial run (A2-B2-C2-D2), and b, d confirmation run (A2-B3-C1-D1)

In the current study, two sample conditions were examined for SEM analysis: the optimized coating (A2-B3-C1-D1) and the initial parameters (A2-B2-C2-D2) which were designated as the mid-level parameters in the Taguchi design. Analysis of surface morphology indicated the presence of an impact coating on both samples. Furthermore, the coating morphology displayed a nodular surface structure at the base, corresponding to the initial Ni-Co-P layer as depicted in Fig 4.3. Additionally, sections resembling flakes were observed above the initial Ni-Co-P layer, attributed to the incorporation of TiO_2 nanoparticles. Consequently, SEM analysis unveiled a distinctive composite coating featuring clearly visible TiO_2-embedded nanoparticles on the surface of the ternary Ni-Co-P coating, reveals the microstructure of the composite coating.

Apart from this, in the other observation the coating of (A2-B2-C2-D2) exhibited certain imperfections (holes) which were rectified in (A2-B3-C1-D1). The possible origin of these imperfections (holes) can be attributed to the

reduction process, leading to the entrapment of hydrogen due to insufficient surface energy. Simultaneously, a new layer is added on the area containing entrapped hydrogen during continuous coating process. However, during stress reliving, the hydrogen trapped within the coating ruptures the surrounding material, creating that hole.

On the other hand, the enhanced parameter configuration of the coating SEM morphology illustrates a seamless microstructure of the coating without any voids, exhibiting a homogeneous dispersion of TiO_2 nanoparticles across the complete area of the Ni-Co-P ternary alloy coating. Within both coatings, the presence of TiO_2 particles is manifested through agglomerates of particles.

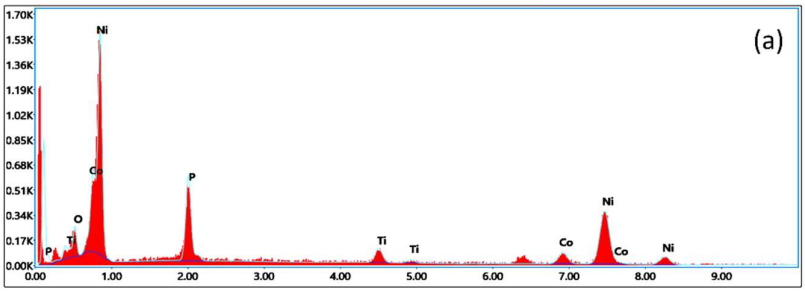

Element	% Weight
O	5
Ni	56.9
P	16.7
Ti	6.5
Co	14.8

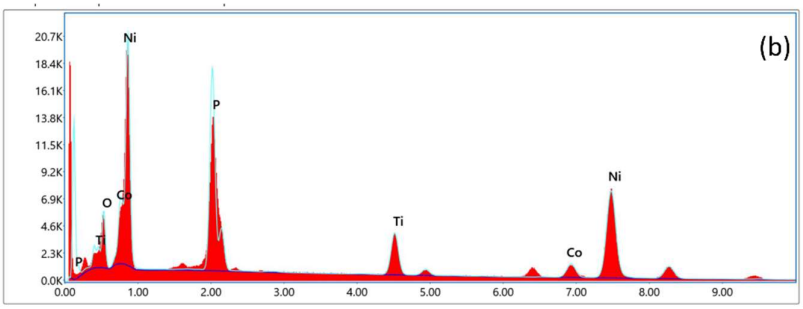

Element	% Weight
O	4.4
Ni	63.4
P	16.6
Ti	8.2
Co	7.4

Figure 4.4: EDS spectrum of Ni-Co-P-TiO_2 composite coatings (a) initial run (A2-B2-C2-D2), and (b)confirmation run (A2-B3-C1-D1)

Refer to Figure 4.4 for further details, The Energy Dispersive Spectroscopy (EDS) value indicates an increment in the deposition of nano TiO_2 content in the optimized (A2-B3-C1-D1) sample. This suggests that the visual analysis through Scanning Electron Microscopy (SEM) can be validated by EDS, demonstrating that in the optimized sample, TiO_2 particles are distributed in more regions and more uniformly compared to the initial state.

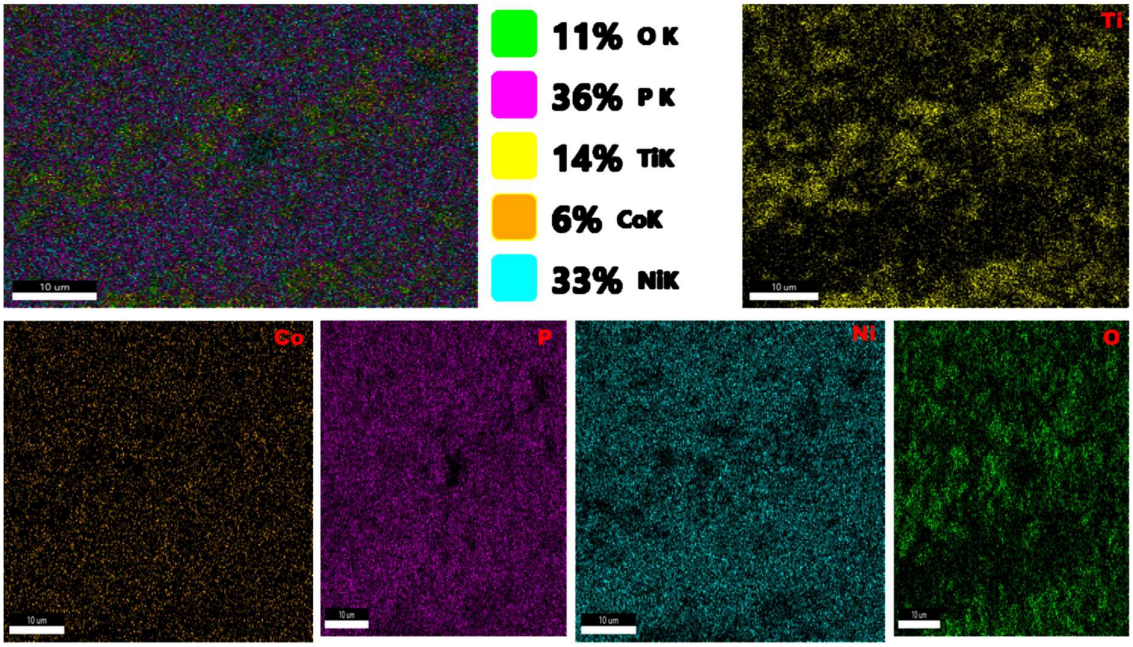

Fig 4.5. Elemental mapping of electroless Ni-Co-P-nanoTiO_2 composite coating.

4.3.4 Morphology of Heat-Treated Ni-Co-P-TiO_2 coatings

Based on the outcomes derived from the Taguchi optimization process, the optimal configuration achieved was identified as (A2-B3-C1-D1). In the current investigation, the optimized coated specimen was subjected to heat treatment at three distinct temperatures namely 200°C, 400°C, and 600°C, in order to gain a more comprehensive insight into the morphological characteristics exhibited by the electroless composite coatings. The morphological features of the Ni-Co-P-TiO_2 coating following heat treatment at 200°C, 400°C, and 600°C are illustrated in Figures 4.6, 4.7, and 4.8, respectively.

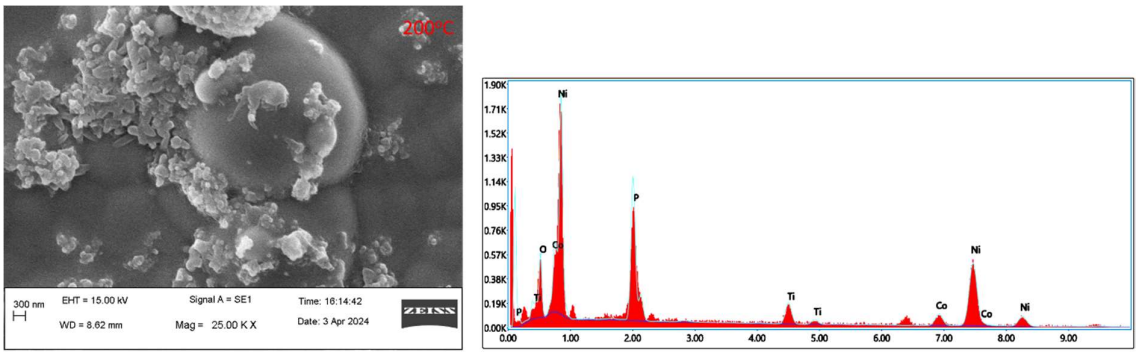

Element	% Weight
O	6.3
P	16.3
Ti	5.7
Co	8.7
Ni	63

Fig4.6: SEM morphology and EDS of heat-treated Ni-Co-P-TiO_2 composite coatings at 200°C.

SEM morphology analysis indicates that there were no discernible alterations observed in the coatings subjected to heat treatment at 200°C, as depicted in Figure 4.6. The morphology of the coatings appears to be similar to that of the as-coated Ni-Co-P-TiO_2 electroless coated samples, as illustrated in Figure 4.3.

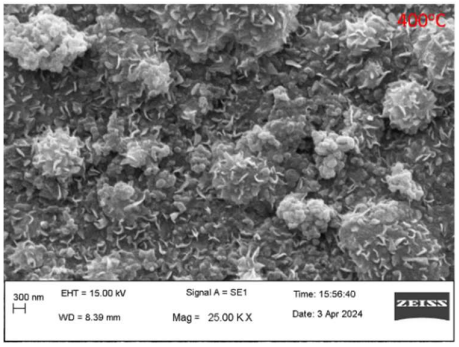

Element	% Weight
O	9
P	13.6
Ti	3
Co	9.5
Ni	65

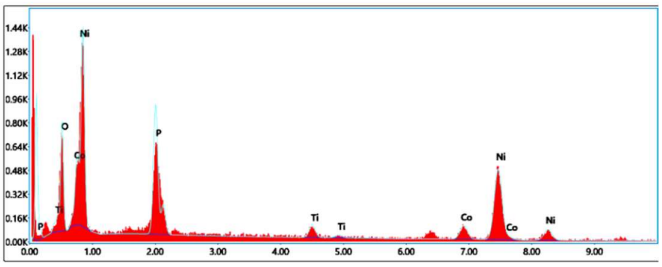

Figure 4.7: SEM morphology and EDS of heat-treated Ni-Co-P-TiO2 composite coatings at 400 °C.

Nevertheless, with reference to Figure 4.7, the morphology of Ni-Co-P-TiO_2 after undergoing heat treatment at 400°C exhibit a significantly enlarged nodular structure, along with a nanoporous surface appearance. Additionally, grain recrystallization is observed at the same temperature. Furthermore, the morphology of Ni-Co-P-TiO_2 after heat treatment at 600°C, as depicted in Figure 4.8, reveals a heightened presence of nodules, manifesting as sheet-like or flaky structures due to the elevated temperature treatment. Moreover, the specimen treated at 600°C displays imperfections such as voids.

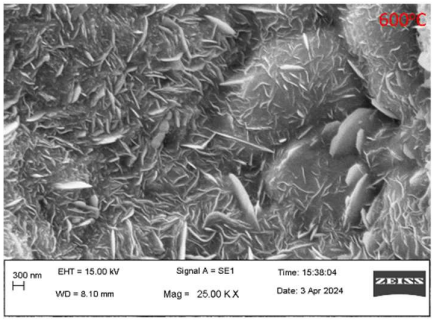

Element	% Weight
O	31.2
P	14.9
Ti	1.4
Co	49.6
Ni	2.9

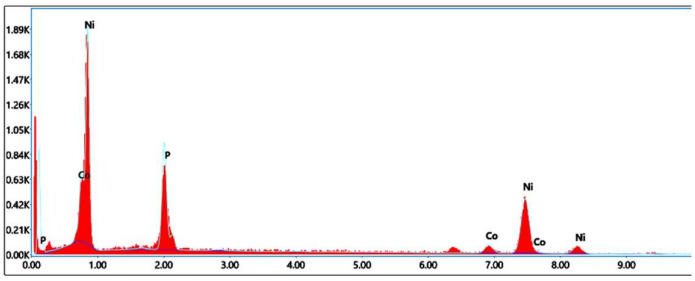

Figure 4.8: SEM morphology and EDS of heat-treated Ni-Co-P-nanoTiO_2 composite coatings at 600°C

4.3.5 XRD Analysis

The X-ray diffraction (XRD) analysis was conducted on the as-coated coating optimized at (A2-B3-C1-D1) and the sample subjected to heat treatment at 400ºC, as illustrated in Figure 4.8 (a), (b). A matching software was utilized to correlate peak positions with specific crystal planes, and the corresponding JCPDS number was determined based on the software's output.

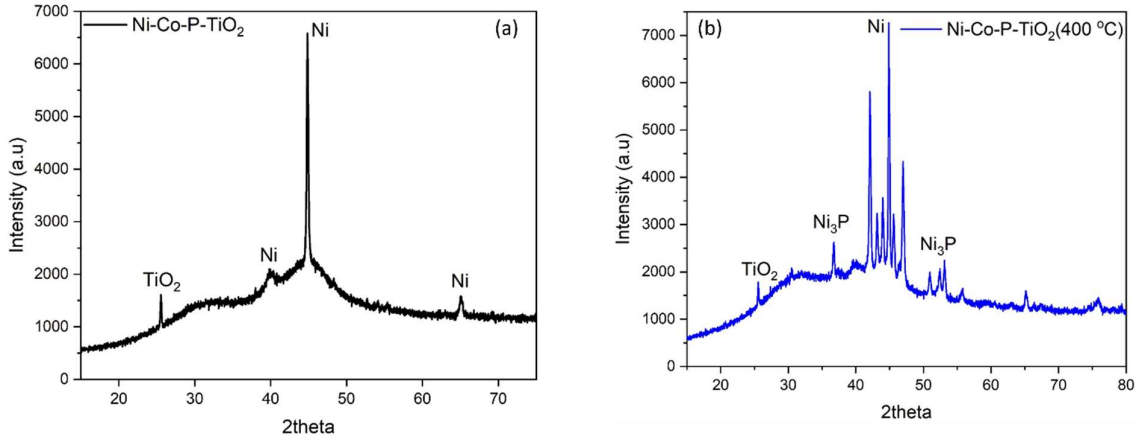

Figure 4.8: XRD of as-plated (A2-B3-C1-D1) and heat treated (at 400ºC) Ni-Co-P-TiO_2 composite coatings.

The XRD profiles demonstrate a semi-crystalline nature, indicating a combination of crystalline and amorphous phases within the as-plated coated sample illustrated in Fig. 4.8 (a). In contrast, the XRD profile of the heat-treated sample depicted in Fig. 4.8(b) exhibits distinct and highly intense crystalline peaks. Both the coated samples (Heat treated and Optimized) yielded a broad range of angles (2θ) centred around 45°, corresponding to Ni (111). Fig. 4.8(b) highlights the formation of an Ni_3P phase on the coated sample due to grain recrystallization at 400 °C, as evidenced by the XRD profile of the heat-treated sample.

Moreover, in addition to the Ni (111) and Ni3P phase, there is an additional weak peak located at approximately 2θ = 25.5°, confirming the existence of TiO_2 corresponding to JCPDS number 96–500-0224. The presence of a minute TiO_2 peak is attributed to the dispersed distribution of nanoparticles in the coatings. The crystal structure of TiO2 reveals the 011 plane within a tetragonal system, where the unit cell parameters are a = b = 3.7892 Å and c = 9.5370 Å. This observation provides evidence that TiO_2 nanoparticles have been integrated into the Ni-Co-P matrix to produce Ni-Co-P-TiO_2 composite coatings.

Chapter 5:

Summary and Concluding Remark

5.1 Conclusion

Electroless deposition of a quaternary Ni-Co-P-TiO_2 coating on a mild steel substrate was conducted within an acidic environment. The experimental design was meticulously structured through the consideration of four key parameters, namely Nickel Source Concentration, Reducing Agent Concentration, Cobalt Source concentration, and TiO_2 nanoparticle concentration, employing the Taguchi Design methodology. The study focused on evaluating the "Hardness". Statistical analysis was performed on all four parameters to ascertain their individual significance. The analysis yielded the following outcomes:

- The Taguchi method determined that the optimal parameter combination for achieving maximum Hardness is A2-B3-C1-D1.
- Through Taguchi analysis, it was established that Nickel Sulphate exerts the most pronounced effect.
- The highest observed Hardness was $425HV_{0.025}$. However, run number 6 demonstrating the highest hardness within the L9 orthogonal array.
- The enhancement of the coating's hardness under the optimal parameters was observed to increased that of the substrate hardness.
- Some imperfections were identified in the initial coating, which were rectified in the coating under optimal parameters.
- XRD analysis indicated that the coating possesses a semi-crystalline nature.

5.2 Future Scope of Work

In the current investigation, a Ni-Co-P-TiO_2 composite coating was formulated through electroless deposition, with a specific focus on the impact of coating parameters for the enhancement of hardness. Nonetheless, there exists a substantial scope for prospective research endeavours, outlined as follows:

- To study the surface roughness characteristics exhibited by Ni-Co-P-TiO_2 coatings.
- Exploring the wear resistance properties of Ni-Co-P-TiO_2 coatings.
- Assessing the corrosion resistance of Ni-Co-P-TiO_2 coatings.
- Analysing the wettability of Ni-Co-P-TiO_2 coatings.
- Conducting characterization through Nano-indentation and Transmission Electron Microscopy (TEM) of the Ni-Co-P-TiO_2 coatings.
- Investigating the deposition rate and coating thickness of Ni-Co-P-TiO_2 coatings.
- Integrating the Taguchi methodology with Grey relation analysis to achieve multi-objective optimization of the process parameters.

Reference

[1] Shi, L. T., Hu, J., Fang, L., Wu, F., Liao, X. L., & Meng, F. M.. (2016). *Effects of cobalt content on mechanical and corrosion properties of electroless Ni-Co-P/TiN nanocomposite coatings*. *67*(10). https://doi.org/10.1002/MACO.201608844

[2] Zhao, Q., Liu, C., Su, X., Zhang, S., Song, W., Wang, S., Ning, G., Ye, J., Lin, Y., & Gong, W.. (2013). *Antibacterial characteristics of electroless plating Ni–P–TiO2 coatings*. *274*. https://doi.org/10.1016/J.APSUSC.2013.02.112

[3] Shoeib, M. A., Kamel, M. M., Rashwan, S. M., & Hafez, O.. (2015). *Corrosion behavior of electroless Ni–P/TiO2 nanocomposite coatings*. *47*(6). https://doi.org/10.1002/SIA.5764

[4] Shoeib, M. A., Kamel, M. M., Rashwan, S. M., & Hafez, O.. (2015). *Corrosion behavior of electroless Ni–P/TiO2 nanocomposite coatings*. *47*(6). https://doi.org/10.1002/SIA.5764

[5] Chen, W., Gao, W., & He, Y.. (2010). *A novel electroless plating of Ni–P–TiO2 nano-composite coatings*. *204*(15). https://doi.org/10.1016/J.SURFCOAT.2010.01.032

[6] Seifzadeh, D., & Rahimzadeh Hollagh, A.. (2014). *Corrosion Resistance Enhancement of AZ91D Magnesium Alloy by Electroless Ni-Co-P Coating and Ni-Co-P-SiO2 Nanocomposite*. *23*(11). https://doi.org/10.1007/S11665-014-1210-6

[7] Kongkidakarn, T., Sawai, D., & Yuttanant, B.. (2014). *Effects of Co content and heat treatment on mechanical properties of electrolessly deposited Ni-Co-P alloys*. *46*(4). https://doi.org/10.1002/SIA.5410

[8] Sarkar, S., Baranwal, R. K., Biswas, C., Majumdar, G., & Haider, J.. (2019). *Optimization of process parameters for electroless Ni–Co–P coating deposition to maximize micro-hardness*. *6*(4). https://doi.org/10.1088/2053-1591/AAFC47

[9] Sarkar, S., Baranwal, R. K., Mukherjee, A., Koley, I., Biswas, C., Haider, J., & Majumdar, G.. (2020). *Optimisation & minimisation of corrosion rate of electroless Ni-Co-P coating*. *6*(3). https://doi.org/10.1080/2374068X.2019.1709326

[10] Sankara Narayanan, T. S. N., Selvakumar, S., & Stephen, A.. (2003). *Electroless Ni–Co–P ternary alloy deposits: preparation and characteristics*. *172*(2). https://doi.org/10.1016/S0257-8972(03)00315-3

[11] Liu, W.-L., Hsieh, S. H., Chen, W.-J., & Hsu, Y. C.. (2009). *Growth behavior of electroless Ni–Co–P deposits on Fe*. *255*(6). https://doi.org/10.1016/J.APSUSC.2008.10.073

[12] Yongjin, G., Huang, L., Zheng, Z. J., Li, H., & Zhu, M.. (2007). *The influence of cobalt on the corrosion resistance and electromagnetic shielding of electroless Ni Co P deposits on Al substrate*. *253*(24). https://doi.org/10.1016/J.APSUSC.2007.06.010

[13] Banerjee, T., Sen, R. S., Oraon, B., & Majumdar, G.. (2013). *Predicting electroless Ni–Co–P coating using response surface method*. *64*(9). https://doi.org/10.1007/S00170-012-4136-X

[14] Kumar, A., Suhag, A. K., Singh, A., Sharma, S. K., Kumar, M., & Kumar, D.. (2014). *Deposition and characterization of amorphous electroless Ni-Co-P alloy thin film for ULSI application*. *1*(3). https://doi.org/10.1088/2053-1591/1/3/035007

[16] Kumar, A., Singh, A., Kumar, M., Kumar, D., & Barthwal, S.. (2011). *Study on thermal stability of electroless deposited Ni-Co-P alloy thin film*. *22*(9). https://doi.org/10.1007/S10854-011-0336-7

[17] Yan, Y., Tian, Y., Hao, M., & Miao, Y.. (2016). *Synthesis and characterization of cross-like Ni-Co-P microcomposites*. *111*. https://doi.org/10.1016/J.MATDES.2016.08.094

[15] Kumar, A., Kumar, M., & Kumar, D.. (2010). *Deposition and characterization of electroless Ni-Co-P alloy for diffusion barrier applications*. *87*(3). https://doi.org/10.1016/J.MEE.2009.06.034

[18] Wang, Y., Shu, X., Gao, W., Shakoor, R. A., Kahraman, R., Yan, P., Lu, W., & Yan, B.. (2015). *Microstructure and properties of Ni–Co–TiO2 composite coatings fabricated by electroplating*. *29*. https://doi.org/10.1142/S0217979215400081

[19] Xie, Z.-H., Yu, G., Hu, B., Lei, X., Li, T., & Zhang, J.. (2011). *Effects of (NH4)2SO4 on the characteristics of the deposits and properties of an electroless Ni–P plating solution*. *257*(11). https://doi.org/10.1016/J.APSUSC.2011.01.016

[20] Mitra, A.. (2011). *The Taguchi method*. *3*(5). https://doi.org/10.1002/WICS.169

[21] Nandagopal, K., & Kailasanathan, C.. (2016). *Analysis of mechanical properties and optimization of gas tungsten Arc welding (GTAW) parameters on dissimilar metal titanium (6Al4V) and aluminium 7075 by Taguchi and ANOVA techniques*. *682*. https://doi.org/10.1016/J.JALLCOM.2016.05.006

[22] Mandal, B., Kumar, V., & Oraon, B.. (2023). *Optimization, Prediction, and Characterization of Electroless Ni-W-P-nanoTiO2 Composite Coatings on Pipeline Steel*. https://doi.org/10.1007/s13369-023-07928-0

[23] Optimization of Milling Process Parameters of En33 Using Taguchi Parameter Design Approach

[24] Seikh, A. H., Mandal, B. B., Sarkar, A., Baig, M., Alharthi, N. H., & Alzahrani, B.. (2019). *Application of response surface methodology for prediction and modeling of surface roughness in ball end milling of OFHC copper*. *14*(1). https://doi.org/10.1186/S40712-019-0099-0

[25] Kim, S.-T., Park, M.-S., & Kim, H.-M.. (2004). *Systematic approach for the evaluation of the optimal fabrication conditions of a H2S gas sensor with Taguchi method*. *102*(2). https://doi.org/10.1016/J.SNB.2004.04.029

[26] Ayoubi, B., Soleimani, D., & Sheydaei, M.. (2019). *Taguchi method for optimization of immobilized Dy2O3/graphite/TiO2/Ti nanocomposite preparation and application in visible light photoelectrocatalysis process*. *849*. https://doi.org/10.1016/J.JELECHEM.2019.113377

[27] Daneshvar, N., Khataee, A. R., Rasoulifard, M. H., & Pourhassan, M.. (2007). *Biodegradation of dye solution containing Malachite Green: Optimization of effective parameters using Taguchi method*. *143*(1). https://doi.org/10.1016/J.JHAZMAT.2006.09.016

[28] Seikh, A. H., Mandal, B. B., Sarkar, A., Baig, M., Alharthi, N. H., & Alzahrani, B.. (2019). *Application of response surface methodology for prediction and modeling of surface roughness in ball end milling of OFHC copper*. *14*(1). https://doi.org/10.1186/S40712-019-0099-0

[29] Erdemir, F.. (2017). *Study on particle size and X-ray peak area ratios in high energy ball milling and optimization of the milling parameters using response surface method*. *112*. https://doi.org/10.1016/J.MEASUREMENT.2017.08.021

[31] Sudagar, J., Lian, J., & Sha, W.. (2013). *Electroless nickel, alloy, composite and nano coatings – A critical review*. *571*(571). https://doi.org/10.1016/J.JALLCOM.2013.03.107